

The authors would like to thank the reviewers of the manuscript entitled “Evaluation of the accuracy of thermal dissociation CRDS and LIF techniques for atmospheric measurement of reactive nitrogen species” for their helpful comments and suggestions. Our responses are as follows. The reviewer comments are in italics, our responses are in regular font, and changes to the manuscript are in blue.

5

Reviewer #1

P2L25 Methods that detect some individual components of NO_y are listed. How were they selected? Why not include e.g. NO₃ or HONO etc

10 We wanted to highlight the detection of the just the largest components of reactive nitrogen. However, based on the feedback from both Reviewer 1 and 2, we have expanded this section to include references to NO₃, HONO, and other detection techniques for organic nitrates. **P2L28** now reads: “HONO has been detected by long path differential optical absorption spectroscopy (Perner and Platt, 1979) and NO₃ has been detected by CRDS (King et al., 2000).”

15 **P3L24** “For example, TD-LIF detects NO₂ at low pressure following thermal dissociation, which minimizes secondary recombination reactions of the dissociated radicals”. Are TD-LIF instruments always operated with the oven at low pressure which would minimise the recombination by reduction of reaction time and rate coefficient?

20 TD-LIF instruments are sometimes operated with the oven at low pressure, but not always. In this sentence, we meant that the NO₂ detection (i.e. in the optical cavity, not the oven) always happens at low pressure, but have updated it for clarity. **P3L26** now reads: “For example, TD-LIF detects NO₂ at low pressure following thermal dissociation. Secondary recombination reactions of the dissociated radicals would thus be suppressed in the detection region, although the thermal dissociation inlet may be operated at either high or low pressures in these instruments. However, it is subject to interferences from ambient levels of NO and NO₂...”

25 **P3L29** “TD-CRDS is an absolute measurement....” Does TD-CRDS being based on a cross-section of NO₂ really make it absolute? As stated later in the manuscript, the effective optical path-length needs to be calibrated by adding known amounts of NO₂. Also, the TD-inlet is part of the instrument and its dissociation efficiency needs to be calibrated (the subject of this paper).

30 The CRDS measurement does not require calibration of the instrument response; it relates the ringdown time directly to concentration through equation (2), in which the calibration is an absorption cross section, making it an absolute measurement. The instrument is periodically compared to an NO₂ standard, but remains absolute. While characterization of the effective optical cavity length, R_L, is required, it is not necessary to use NO₂ for this process. Any gas-phase species which absorbs at 405 nm would allow us to measure this, it just happens that NO₂ is the most convenient. As for the TD-inlet, as long as the temperature setpoint is set correctly, no calibrations are required since the conversion efficiency should be a constant. Standard additions of specific NO_y components would then still be useful for validation of instrument performance. The reviewer raises a good point that perhaps a better word for these steps is “characterization”, rather than “calibration”. We have updated the lines in the experimental and discussion sections to reflect this. **P5L29** now reads: “ σ/R_L is characterized regularly by filling the cavity with several different known NO₂ concentrations.” **P20L5** now reads: “TD ovens should be characterized with the appropriate reactive nitrogen compounds regularly at the oven set points using the oven residence time and gas pressure that will be used in ambient sampling.”

35 **P4L3** “though this reaction rate depends on the TD inlet pressure and flow rate”. What reaction rate is this referring to (NO + O₃ makes NO₂ but O + NO₂ or NO does not)?

40 The Wooldridge *et al.* paper was referring to the O₃ + NO reaction (among others) when it said these interferences are subject to pressure, so this is the reaction we were referring to. For clarity, we have removed the phrase “(or the O atoms that form in O₃ pyrolysis)” from the manuscript to clarify that we

are referring to the $O_3 + NO$ reaction. P4L5 now reads: “Likewise, ambient levels of O_3 in the sampled air may react in the oven with NO to form NO_2 , resulting in a positive bias (Pérez et al., 2007), though this reaction rate depends on the TD inlet pressure and flow rate (Wooldridge et al., 2010)”

5 P4L10 “Thieser et al. (2016) parameterized the bias in peroxyacetyl nitrate and 2-propyl nitrate detection in their inlet as a function of ambient NO and NO_2 concentrations, but noted that these parameterizations may vary for other PN or ANs. These effects are generally considered minor compared to other uncertainties in the measurement”. Is this true? In some TD-instruments, depending on operating temperature, the effects of radical recombination ($RO_2 + NO_2$) or oxidation of NO ($RO_2 + NO$) can bias the detection of peroxy nitrates by factors of 2 or more and is likely the biggest source of uncertainty.

10 Thanks to the reviewer for pointing out this sentence was unclear. It was intended to refer to all the interferences described in this paragraph, and it was also intended to refer to after the biases were removed. However, we don't wish to speak for the authors of those papers, and we have therefore deleted 15 that phrase.

15 P6L11 Does the temperature probe measure the gas-temperature or the temperature of the inner wall of the quartz tube? Can there be different due to gradients from the centre of the tube to the wall?

20 The temperature probe is mounted on the outside of the quartz. As we point out on P6L12, the effect is that the actual gas temperature is slightly higher than the temperature setpoint, however, we periodically monitor the gas temperature by inserting a temperature probe into the oven, as seen in Fig. S1.

P6L17 Does addition of 30 ppmv O_3 have any adverse effects? Can e.g. ozonolysis of biogenics take place 25 in this volume? Might this form particles or radicals (Criegees) than can react with NO_2 ?

No, we are not concerned with this. Ozonolysis is quite slow, typically on the order of $10^{-17} \text{ cm}^3/\text{molec/s}$. 30 Even though the ozone concentration may be high, the concentration of unsaturated hydrocarbons which may undergo ozonolysis is typically at the level of a few ppbv or less. We would therefore expect less than 0.5% conversion, or an interference on the order of ~20 pptv, which is below the detection limit.

P8L7 “A custom-built iodide adduct chemical ionization mass spectrometer (Lee et al., 2014), described 35 in further detail in (Veres et al., 2015), was used to monitor the N_2O_5 and HNO_3 concentrations” How was the CIMS calibrated? How accurate are the concentration measurements?

As detailed in the paragraph starting on P14L19, the CIMS was calibrated for HNO_3 using a permeation tube, but no calibration source was available for N_2O_5 , so a relative measurement was obtained. The 40 CIMS measurements are accurate to within 20-25%. P8L12 now reads: “This measurement has a detection limit of 4 pptv and 70 pptv and error bars of 25% and 25% (3σ) for N_2O_5 and HNO_3 , respectively.”

P8L25 What is the pressure in the Berkeley oven? What are the standard operating conditions for this 45 instrument. I believe it has been operated using different pressure configurations.

The Berkeley TD-LIF instrument had an oven operating at ambient pressure, as described in Day et al (2002). P8L27 now reads: “ HNO_3 and n-propyl-nitrate samples were provided by permeation tubes similar to those described in Sect. 2.2, diluted in dry zero air, and passed through 20 cm heated length quartz ovens, held at ambient pressure, at a flow rate of 2 slpm.”

50 P8L16 The modelling of this system is not trivial. As the authors state, many rate constants have not been measured at the higher temperatures. Secondly, the authors do not consider surface catalysed thermal decomposition, which is important as the authors mention briefly later when discussing the low temperature NOy instruments with catalytic conversion at the metal surfaces. The wall losses of radicals is probably the biggest uncertainty and can only be assessed by variation of experimental parameters. Thieser et al. 2016 showed that variation of the concentration of the organic nitrates they were using (and thus variation of the RO_2 concentration) affected the loss rate, which could then be explained using

a Langmuir-Hinshelwood type expression. Did you change the concentration (e.g. of HNO_3) significantly to see if the same wall loss rate constant was appropriate? Do you expect the rate constant for wall loss to be independent of temperature (effects of diffusion, turbulent mixing)?

We did not change the concentration of HNO_3 , because we were limited by the output of the permeation tube, which, at a flow rate of 1.9 slpm provided a maximum mixing ratio of ~5 ppbv. We used this maximum concentration because it is where we would expect the highest probability of recombination. While we expect the effect of recombination to be even lower at more diluted concentrations, we didn't explicitly test conversion efficiency as a function of HNO_3 concentration. We have inserted a line stating this caveat. P10L24 now reads: "No attempt was made to dilute the output of the HNO_3 permeation tube any further, as recombination effects would likely only be less important at lower starting HNO_3 concentrations."

P9L23 was the HNO_3 input mixing ratio based on the permeation source or the CIMS signal?

It was based on the output of the permeation source. The CIMS signal is also calibrated on the output of the permeation source, so to base the calculation on CIMS signal would introduce more error into the calculation.

P9L31... "possible due to recombination reactions....." Which ones? Be specific.

We have clarified that the recombination reaction is of OH and NO_2 . P10L5 now reads: "The 0.5 slpm thermogram has a slightly lower maximum conversion efficiency (95%), possibly due to the recombination reaction of OH and NO_2 during the extended time in the cool down region prior to detection."

P10L8 High and low pressure limits have been used to calculate the thermal dissociation rate constant for HNO_3 . What value for F_c was used to calculate the rate coefficient at 500° C. Also, Glänzer and Troe did their study in Argon. Are the results applicable for air (what is the relative collisional stabilisation efficiency)?

We used a value of $F_c = 0.6$, and have put a note in Table S1 stating this. Following the example of Day et al (2002), we didn't attempt to make any correction for air vs. argon. To our knowledge, no studies of the HNO_3 thermal decomposition were conducted in air. Wine et al (JCP 1979) measured the recombination reaction in Ar and N_2 and found that although there was a ~30% difference in the rate constant at room temperature (at ~20 Torr), that difference decreased to 10% at 350K. They did not do any experiments at higher temperatures or at ambient pressure. So given the basic nature of the kinetic model, we didn't attempt to make a corrective factor.

P10 L13 "...the recombination rate for $\text{OH} + \text{NO}_2$ is quite low..." Be quantitative. What is the rate coefficient at this temperature and what is the pseudo-first order rate coefficient for recombination for a given NO_2 level of e.g. 10 ppbv. This can then be compared to the wall loss rate coefficient.

The rate constant at 650 °C is on the order of $3 \times 10^{-13} \text{ cm}^3 \text{ molec}^{-1} \text{ s}^{-1}$. Therefore, the pseudo-first order rate coefficient for recombination, given an NO_2 level of 10 ppbv is ~0.075 s⁻¹, nearly three orders of magnitude lower than the wall loss rate coefficient of 46 s⁻¹. We have inserted a line which describes this. P10L21 now reads: ...OH radicals are far more likely to be lost to the walls of the oven (at a diffusion-limited rate determined by Day et al. (2002) of ~46 s⁻¹ for 1/4" OD tubing, which is far higher than the pseudo-first order recombination rate coefficient of 0.075 s⁻¹ at $[\text{NO}_2] = 10 \text{ ppbv}$).

P10L27 Did Sobanski et al. (2016) also present a decomposition efficiency for HNO_3 ? Are the results comparable? Note that Sobanski et al used a radical scavenger with a large surface to reduce radical recombination in the heated inlet.

They presented a decomposition efficiency curve up to 350 °C, and found the HNO_3 conversion efficiency was close to 0% at these temperatures. This is consistent with our results, and we have inserted that reference into the manuscript. P10L29 now reads: This is in contrast to ANs and PNs, for which the

reaction of the dissociated peroxy and alkyl radicals with NO_2 is a significant interference (Thieser et al., 2016), but in good agreement with the HNO_3 results of Day et al. (2002) and Sobanski et al. (2016).

P11L9 “.. the onset and final conversion of HNO_3 are not strongly sensitive to pressure”. Is this because 5 wall losses are invariant with pressure? is the conclusion that wall losses are so large that recombination never compete ? What if the sample contains not only HNO_3 but also NO_2 to increase the rate of reformation of HNO_3 ? The authors should consider doing one such experiment to see if elevated NO_2 will influence the shape of the HNO_3 thermogram. The same applies to the NH_3 experiments.

Yes, that is our conclusion. If we calculate the pseudo-first order rate coefficient for recombination with 10 $[\text{NO}_2] = 50 \text{ ppbv}$, which is much higher than typically observed in the field, that rate coefficient is still two orders of magnitude lower than the wall loss rate coefficient, and is still unlikely to compete. We agree that testing this experimentally would be an interesting direction to take these studies in the future, but such tests were not feasible at this time. However, the kinetic box model supports this hypothesis, and 15 we have inserted a line indicating this. P10L26 now reads: “Similarly, increasing the starting NO_2 concentration, to mimic conditions in highly polluted environments, was not attempted in this set of experiments, but increasing the starting NO_2 concentration in the kinetic model up to 50 ppbv shows that there is no recombination expected even with elevated NO_2 in the oven.”

P11L26 This sentence implies that the modelling done in this study (which considers gas-phase processes 20 only) is only a partial representation of the chemistry going on. As mentioned above, the sensitivity HNO_3 detection while adding NO_2 would have been useful to confirm that the simple model reproduces the thermograms for the right reasons.

Please see our response to the previous comment.

P12L11 The data shows that the VOCs added had no effect. Not surprising considering their bond-dissociation energies. It would have been more informative to have added VOCs that will decompose, 25 especially organic nitrates as they result in more complex radical chemistry and NO_x .

The purpose of the VOC additions were to test the effect on the secondary chemistry of HNO_3 conversion 30 in high VOC environments, such as the recent Uintah Basin Winter Ozone Studies (see Wild 2016), where thermal dissociation inlets were used to measure NO_y and speciated NO_y . While the reviewer is correct that adding organic nitrates would also be interesting, the scope this paper was limited to the listed components of reactive nitrogen, HNO_3 , N_2O_5 and ammonium nitrate, to test quantitative conversion at high temperature. However, the study of Thieser et al. nicely defines the effect of organic nitrates. We 35 have inserted a line clarifying the intention of these experiments. P12L23 now reads: “Figure 5b shows the measured thermogram with the addition of ~50 ppbv VOCs (described in Sect. 2.2) with and without the addition of 90 ppbv O_3 , as well as the addition of 5 ppmv of propane, to mimic conditions found in highly polluted wintertime atmospheres.”

P12L17 “....The oven is set at sufficiently high temperatures to dissociate ANs and PNs back to NO_2 + 40 the organic radical” Not true. At higher temperatures the RO_2 formed from thermal dissociation of PNs is unstable (see Thieser et al. 2016).

The reviewer is correct, RO_2 is often unstable at high temperatures. We were intending to say that if some 45 RO_2 formed via ozonolysis or other mechanism, it is unlikely that it would scavenge NO_2 to reform PNs, since PNs would immediately dissociation. It is true that if the RO_2 simply dissociated, then it wouldn’t react with NO_2 at all. Therefore, we have inserted a line which states that the RO_2 molecule would be more likely to dissociate. P12L30 now reads: “Reactions of unsaturated hydrocarbons with O atoms or OH radicals tend to be rapid and would produce organic radicals, but these tend to be unstable, and any stable radicals would likely only react with NO_2 to form ANs or PNs. The oven is set at sufficiently high temperatures to dissociate ANs and PNs back to NO_2 + the organic radical.”

P12L27 "...The dominant reaction of O_3 in the model is the reaction with NO_2 to make NO_3" Is this true? I would have thought the pyrolysis will dominate at high temperatures. Is the O_3 pyrolysis rate constant in the model correct? What is the O -to- O_3 ratio at thermal and kinetic equilibrium?

We have changed the line to distinguish those reactions from the unimolecular dissociation reaction, which should dominate at higher temperatures. P13L9 now reads: "The dominant bimolecular reaction of O_3 in the model is the reaction with NO_2 to make NO_3 , but since these reactions are occurring at high temperature, any NO_3 formed will immediately dissociate to NO_2 (see Sect. 3.2)."

P12L30 The reaction between O and NO_2 does not form much NO_3 but mainly $NO + O_2$. This is especially true at high temperatures.

Both reactions should be relevant, so we have added both to that line. P13L13 now reads: "Of the O atoms that are not lost to the walls, their primary reaction is also with NO_2 to form either $NO + O_2$ or NO_3 but NO should be converted back to NO_2 after the oven."

P13L5 That a model with no surface-catalysed reactions cannot reproduce the effect of a surface catalyzed reaction is not surprising. Why do NO_y instruments with e.g. gold-surfaces see decomposition at much lower temperature than needed to break the $HO-NO_2$ bond and why do they add CO ? It is more than "possible" that surface reactions play a role, it is rather clear.

We have removed the word possible, and replaced it with the word "likely". P13L25 now reads: "It is likely that there is some surface reaction that affects the HNO_3 conversion in the presence of CO ."

P16L25 Are there any other reactions of NH_2 that should be considered. Could it react with NO or NO_2 ?

Thanks for noticing this. Although the $NH_2 + NO$ and $NH_2 + NO_2$ reactions were included in the model, they were mistakenly omitted from table S1. They have now been included.

P17L6. "However, even this rudimentary simulation predicts the general shape of the experimental data..." What aspect of the "general shape" does it reproduce? Perhaps you can be more concise here.

We have changed the line to be more specific. P17L24 now reads: "This rudimentary simulation predicts the initial signal increase starting at 300 °C, though it has a maximum conversion efficiency of just under 2%, which is below that observed in the experiment."

P18L3 "ambient levels of a group of representative VOCs". As already mentioned, addition of VOCs that are unstable at the inlet temperatures (organic nitrates) would have been more informative.

Please see our response to the comment on line P12L11.

P18L23 "... N_2O_5 is not typically considered in the TD- NO_2 instrument literature because the existing instruments have largely operated in the daytime..." Perhaps this statement is too general. Some instruments measure day and night and have considered effects of N_2O_5 thermal decomposition (e.g. Thieser et al. 2016)

That is true, there are some groups which have used TD inlets at night. We have rewritten that paragraph to incorporate this. P19L5 now reads: "TD- NO_y instruments often operate in the daytime when N_2O_5 is not a significant fraction of NO_y , though some groups have operated at night and have typically assumed complete conversion to $NO_2 + NO_3$ at the TD inlet setpoint for PNs (Di Carlo et al., 2013), and complete conversion to $2NO_2 + O$ at the setpoint for HNO_3 (Wild et al., 2014). These results confirm that there is approximately quantitative conversion at these setpoint, though there are slight deviations from 100% conversion near the PN setpoint. Therefore, care must be taken to select a setpoint carefully and ensure complete conversion at that temperature. However, this interference would only be significant during nighttime or during very cold weather sampling."

P18L32 "...These results demonstrate that the volatile portion of the particulate nitrates will be driven into the gas phase at low oven temperatures.." Particulate nitrate is not only ammonium nitrate but has a large component of organic nitrates. At which efficiency will these be detected?

While we agree that organic nitrates are of significant interest, ammonium nitrate, which is in equilibrium with HNO_3 in the atmosphere, was the target of this study. We have inserted a line clarifying that we are talking about particulate ammonium nitrate. We have also inserted a line saying that although it's possible that other organic nitrates would behave similarly, further experiments would be required to test this.

5 **P19L22** now reads: "These results demonstrate that the volatile portion of the particulate ammonium nitrates will be driven into the gas phase at low oven temperatures, consistent with Rollins et al. (2010), who used a denuder to remove gas phase nitrates and to detect aerosol organic nitrates in a 325 °C oven. Their results indicate it is likely that particulate organic nitrates would be converted to NO_2 with 100% efficiency in the NOAA TD-CRDS, but this result has not been explicitly tested here."

10

Technical / typographical

P2L20 Techniques that detect the major individual components of NOy include detection....

See response to P2L20 above

15 **P4L1/3** negative / positive artefact = negative / positive bias?

We have changed the word artifact to bias on P4L5 and P4L7.

P5L4 Inappropriate reference. Fuchs et al were not the first to use CRDS for atmospheric trace gases as this implies.

20 The intent was to cite a representative reference, not the first reference. We have added a reference at **P5L4** to O'Keefe et al (1988), who were the first that we are aware of to measure ambient NO_2 with CRDS.

P5L18 "light decays" ?

25 We have changed "light decays" to "light decay profiles", for clarity. **P5L18** now reads: "The measured light decay profiles are summed and fit at a 1 Hz repetition rate to yield the ringdown time τ ."

P5L23 "known NO_2 concentrations". How were they determined? Was an "absolute method" used to measure the NO_2 concentration?

30 The known samples of NO_2 were obtained by reacting known amounts of O_3 from an ozone generator with an excess of NO. The ozone generator is a commercial ThermoScientific 49i, which measures O_3 by UV absorption. This is a technique that has been used by our group, and was described in section 2.2 of Washenfelder et al, EST 2011. We have inserted a new phrase to clarify this. **P5L29** now reads: " σ/R_L is characterized regularly by filling the cavity with several different known NO_2 concentrations (obtained by reacting the output of an O_3 standard source with excess NO) and calculating the slope of the measured optical extinction vs $[\text{NO}_2]$ as described in Washenfelder et al. (2011)"

P7L22 "bubbling the dilution zero air through a water bubbler...."

40 We have changed "bubbling" to "passing". **P7L24** now reads: "Water was added by passing the dilution zero air through a water bubbler prior to mixing with the HNO_3 sample."

P8L31 and at several other places in the manuscript. "rate laws" is the wrong term. You refer to "rate constants" or "rate expressions".

These have all been changed to rate expressions (throughout manuscript).

45

References: Several have capitalised manuscript titles. Nikitas et al spelling of Detector.

Thank you for noticing. We have fixed these typos.

Figure captions:

50 *Figure 1: "Instrument schematic of the TD-CRDS instrument" "cool down" (sometimes cooldown" maybe you can find a better expression than "cool down region".*

We have changed this to “cooling region” in the Fig 1 and caption, which is consistent with what Day *et al.* (2002) and Wild *et al.* (2014) have called it.

Figure 3: small dashed line = short dashed line ? Figure 4 “physical oven” ?? Figure 7 “in solid circles” = “as solid circles” ? Figure 8 “shown as red circles” Figure 9 delete preferentially.

We have made these changes.

Supplementary Info: Caption to Fig. S4. “...but if allowed to recombine, only ~40% will be allowed to recombine, but that nearly all O atoms” Not clear what is meant here. Rewrite.

This was a typo/error. We meant to say that only 40% will remain as O₂ + O. Figure S4’s caption now reads: “These results indicate that O₃ dissociates to form O at the entire temperature range relevant for AN and HNO₃ TD ovens, but that if allowed to recombine, only ~40% will remain as O₂ + O. If wall loss is permitted, nearly all O atoms would be lost to reactions with the wall.”

Table S1. Many/most of the reactions listed contribute little to the thermograms (e.g. does neglecting H + NO₃ make any difference at all)? Please highlight those reactions that do have an influence (i.e. those that account for 90 % of the reactive flux). This would make the results of the modelling exercise more transparent. Please add (in a footnote) the original references used for the rate expressions. Just listing the NIST type label (e.g. 1986TSA) is not sufficient. What does JPL ** mean (HNO₃ + OH reaction). Please mark those reactions for which experimental data in the range up to 700 celcius was NOT available and indicate which (if any) are estimated or theoretical.

We have reorganized Table S1. It now includes the rate constant at the minimum and maximum temperature (298K and 950K). We are also now indicating the temperature range, and whether they were experimental or theoretical. References are now directly included. The JPL ** was supposed to be a footnote which was mistakenly omitted, but which is now included. Any reactions at lower than 700 °C were used because reproducible values at higher temperatures were not available.

Reviewer #2

Could the authors explain why they did not carry out experiments using common atmospheric NO_y constituents such as peroxy and alkyl nitrates? Clearly these are likely to fully dissociate at the highest temperatures and this has been shown in previous work on the TD-LIF instrument, however it would have been good to actually see this shown experimentally. A thermogram of n-propyl nitrate from the UC Berkeley TD-LIF instrument is shown but it would have been nice to have seen this for the TD-CRDS system as well (especially considering one of the conclusions from the work is that all ovens behave differently). I do not know if the authors intend to use their system to provide NO_y class speciation in their atmospheric measurements (and hence need to know the thermograms for PNs and ANs), however others may wish to and would therefore be interested to see this.

The reviewer is correct that it is well worth looking at the conversion efficiency of peroxy and alkyl nitrates in a TD-CRDS instrument. Although we do not plan to use the TD inlet at intermediate temperatures for NO_y speciation, others may, and we direct interested readers to the excellent paper by Thieser *et al.* (2016), which covered this topic nicely. We restricted our attention to quantification of the unintended thermal dissociation of HNO₃ at temperatures commonly used to measure ANs, and thus did not attempt to re-measure the conversion efficiency of PNs and ANs.

It would also have been good to have seen the conversion at different levels of NO and NO₂ in the initial sample, corresponding to what would be the case in ambient measurements. Would the authors expect any difference in behavior of the inlet with different NO_x levels (e.g. any NO to NO₂ conversion)?

We appreciate and share the reviewer’s concern. Please see our response to Reviewer #1’s comment on P11L9

Having read the title of the manuscript, I did find myself disappointed at the lack of results shown from the TD-LIF instrument. In reality this seems to be a paper that describes work done on the TD-CRDS system with a single set of results of HNO_3 dissociation from the TD-LIF shown as an example of how two apparently similar systems can behave differently. This is fine and doesn't particularly detract from the results, however maybe the paper title is a bit misleading?

We understand the reviewer's concern, and it is true that this manuscript largely focuses on CRDS, but we would still prefer to retain LIF in the title, as it encompasses the results obtained by two of the paper's coauthors.

I found the section on ammonium nitrate conversion very interesting. It has often been a question when looking at total NOy measurements by some form of conversion to NO or NO_2 as to how much nitrate aerosol is converted and this work goes some way to answer this. I wonder if a recommendation from the work could be that steps should be taken to remove aerosols from the system (e.g. using a cyclone or something similar) if purely gas phase NOy is of interest? Maybe this could also be run sequentially to give an actual measurement of particulate nitrate? Could the authors make any comment on how other particulate nitrate (e.g. organic nitrate) would behave in the system? I would imagine there are situations when organic nitrates could make up a large proportion of the total particulate nitrate and so how these are converted would be of great interest.

Thanks to the reviewer for this suggestion. An impactor or cyclone could be used to eliminate particulate ammonium nitrate, whereas a heated aerosol sampler could potentially be used to sample 100% of the particulate matter in aircraft studies. As for other particulate nitrates, it seems likely that organic nitrates would be driven into the gas-phase with the same efficiency in our oven, given the results of Rollins et al (2010), and therefore would undergo complete conversion, but further tests would be required to test this. We have included lines in the discussion section which address these two issues. P19L24 now reads: "Their results indicate it is likely that particulate organic nitrates would be converted to NO_2 with 100% efficiency in the NOAA TD-CRDS, but this result has not been explicitly tested here." Additionally, P20L1 now reads: "In future studies, a TD inlet that either effectively samples aerosol, or effectively excludes aerosol (such as a cyclone), or a combination of the two could be used to specifically measure aerosol nitrates, which may make up a substantial fraction of NOy, particularly in polluted wintertime urban atmospheres."

Could the authors include a summary plot showing the thermograms of all the different species? Maybe this would look too busy but it would help the reader to understand the temperature that different conversions and interferences occur.

Yes, we can do this. We have put it in the supporting documents as Figure S8.

Minor corrections:
P2 L20: the authors could also include mention of GC-MS to measure organic nitrates (e.g. Worton et al., *Atmos. Env.* 2010) in their list of NOy techniques.

Thank you for this suggestion. We have included the Worton paper from 2008 which introduced this technique in the introduction. (P2L33)

P4 L19: Are there any examples of using TD followed by photolytic conversion / chemiluminescence to detect the NO_2 ?

As far as we know, the only example of TD-chemiluminescence is Perez et al (2007), which dissociated HONO to make NO. We are not aware of any groups using TD-chemiluminescence to detect NO_2 directly. Because the line referenced here was only discussing techniques which generate NO_2 , we didn't include that reference here, but did include it later in that section.

P5 L28: How are the known concentrations of NO_2 produced (e.g. GPT, standard bottle with dilution)??

Please see our response to Reviewer #1's comment on P5L23

Figure 4: It would be better if these were plotted as a % conversion to NO_2 as is done for all the other figures.

We have changed figure 4 accordingly.

Reviewer #3

5 Main comments and questions:

Page 11, lines 4-13: Placing a stainless steel valve in front of the oven is something that I would avoid working with HNO_3 that may be efficiently loss, even if the authors mention a test with the valve fully opened to check if the conversion of HNO_3 changes when it is removed.

It is true that stainless steel should normally be avoided, but Teflon valves did not provide a stable enough pressure to allow us to use them. Therefore, we used a heated stainless steel valve with the minimum amount of surface area possible to avoid any losses. The thermograms were also run over the course of hours to days, so the HNO_3 should have had enough time to come to an equilibrium with the surface.

15 Page 12, line 3: Authors tested the effect of RH on the thermograph shape of the HNO_3 with a test at 0% and another at 66%. Since in several sites the RH goes up to 90%, it would be worth to have one more point at high RH.

Unfortunately, this would have proved to be technically difficult to achieve, so based on the lack of a difference at 66% RH, we decided not to pursue higher RHs. However, the reviewer is correct that there could possibly be a non-linear water effect that is only evident at very high RHs, so we have included a line which describes this caveat. P12L22 now reads: "Additionally, we did not test the conversion efficiency at very high RH levels, and it's possible there could be a non-linear effect of water."

25 Page 15, lines 7-19: In this paragraph even if not clearly reported, it is implied that the thermal conversion of NH_4NO_3 , reported also in figure 7, is a two step conversion: first from NH_4NO_3 to HNO_3 and then from HNO_3 to NO_2 , since the CRDS measures NO_2 . In this case it would be important the residence time to allow the double thermal dissociation in the heated tube, but this is not mentioned nor explored.

30 We anticipate that the thermal dissociation of NH_4NO_3 , which takes place at much lower temperature, is rapid. Indeed, our model suggests that the thermal dissociation rate of HNO_3 is also quite rapid, and that the residence time in the heater is required largely to effect the temperature rise in the gas sample and not to allow time for the decomposition reactions. Furthermore, the shape of the thermogram, with a plateau at high temperature matching that of HNO_3 , together with the calibration against an NH_4NO_3 source, indicates complete conversion. We added a line indicating this. P16L3 now reads: "The close agreement between the two thermograms demonstrates that the dissociation pathway is $NH_4NO_3 \rightarrow NH_3 + HNO_3$, and that this reaction is rapid at the temperatures reached in the TD inlet."

35 Page 15, lines 17-19 and figure 7: Here it is reported that the thermograph of NH_4NO_3 agrees with that of HNO_3 reported in fig. 2. In fig. 2 are showed 4 thermographs of HNO_3 , but, to me, none of them are the same reported in figure 7.

40 The black trace in figure 7 is the same the one shown in gold squares in figure 4. Thank you for pointing out that this was not clear. The figure caption has been updated as "The black solid line indicates the measured thermogram of gas-phase HNO_3 at a 1.9 slpm flow rate (from the gold squares trace in Fig. 2)."

45 Page 16, line 18: The NH_3 conversion is unimportant for all the TD-LIFs, since all of them measure directly NO_2 : so I would generalize this conclusion to all the TD-LIFs and not only to the Berkeley TD-LIF.

We have made this change. P16L32 now reads: "The interference is only present when O_3 is added to the mixing volume, indicating that the conversion of NH_3 must be producing NO , rather than NO_2 , and is subsequently unimportant to instruments that measure NO_2 only, such as TD-LIF instruments."

Page 18, lines 22-23: This statement is not correct: 1) there are several campaigns where TD- NO_2 were used during nighttime (i.e. BEACHON-RoMBAS, see Fry et al., 2013; RONOCO, see Di Carlo et al., 2013). 2) There is at least one paper where is described that during nighttime the channel of the TD-LIF instrument that converts total peroxy nitrate into NO_2 , converts also N_2O_5 (Di Carlo et al., 2013). In that paper is reported also the comparison of nighttime measured peroxy nitrate by TD-LIF with the N_2O_5 measured by CRDS, taking the advantage of a TD-LIF and a CRDS installed on the same aircraft. In that work it is also showed that the TD-LIF measurements of peroxy nitrated, during nighttime and at least in the RONOCO campaign, are dominated by N_2O_5 .

5 Although the design of TD-LIF instruments has traditionally been oriented toward understanding photochemical reaction products of reactive nitrogen, we agree that the original statement was too general. We have rewritten that paragraph to account for studies that did use TD inlets at night. P19L5 now reads: "TD- NO_y instruments often operate in the daytime when N_2O_5 is not a significant fraction of NO_y , though some groups have operated at night and have typically assumed complete conversion to NO_2 + NO_3 at the TD inlet setpoint for PNs (Di Carlo et al., 2013), and complete conversion to $2NO_2 + O$ at 10 the setpoint for HNO_3 (Wild et al., 2014). These results confirm that there is approximately quantitative conversion at these setpoint, though there are slight deviations from 100% conversion near the PN setpoint. Therefore, care must be taken to select a setpoint carefully and ensure complete conversion at that temperature. However, this interference would only be significant during nighttime or during very cold weather sampling."

20 *Minor comments and questions:*

Page 6, line 1: the inlet tube 0.39 cm ID. Seems too small, is it a typo or a conversion error from inch to cm?

We used $\frac{1}{4}$ " tubing, which has an inner diameter of $5/32" = .39$ cm

25 Page 15, line 5: Cohen, 2016 is cited as reference here, but it is not reported in the reference list.
Thank you for noticing this. Cohen 2016 was indeed missing. [This has been fixed](#).

Comments from Hans Ostoff

30 *Title. The title seems a bit broad given that not all of the major NO_y species were tested (e.g., PAN was not). Also, since measurement accuracy was not actually stated (e.g., "the measurements of are accurate to +/-x%" or something to that effect), perhaps the title should be "Evaluation of interferences of ...?"*

35 We understand Prof. Ostoff's concern, however, because we tested a number of NO_y species, and because we tested them at a wide range of setpoints, not just the ones where they were supposed to be detected (i.e. HNO_3 at the ANs setpoints) we felt that it would be best to state them generally, rather than listing all the species out. Additionally, since the goal was not just to characterize interferences from NH_3 and O_3 additions, but to characterize how effectively the TD inlets convert species such as HNO_3 and 40 ammonium nitrate particles, we would like to retain the phrase measurement accuracy.

pg 1, line 27. *The paper that should be cited for detection of $ClNO_2$ by CRDS is (Thaler et al., 2011).*
Thanks for catching this. [We have fixed the reference](#).

45 pg 3, line 27. *TD-CIMS instruments do not quantify ANs. They are usually quantified by clustering reactions with iodide and do not utilize a TD inlet.*

This is true. We should not have included ANs in the list of species TD-CIMS detects. [We have removed ANs from that line](#).

50 pg 7, line 3. *Typo (Marrin)*
[We have fixed this typo](#).

pg 9, lines 21-22, and all figure captions. Please specify which instrument was used to monitor NO_2 . It was not always obvious.

5 We have clarified that in all cases except when we are discussing the Berkeley TD-LIF, the NOAA TD-CRDS instrument was measuring NO_2 . (Throughout manuscript)

pg 10, line 27. Sobanski (2016) is not listed in the reference section.

The reference is now listed.

10 pg 11, line 25. "The Berkeley group has found the HNO_3 conversion to be oven dependent even for identical pressure and flow conditions indicating some but not all ovens have impurities at the walls that effectively catalyze HNO_3 decomposition." This statement has major implications and should perhaps be featured more prominently (maybe repeated in the conclusion section). Can the authors speculate as to what these impurities might be? How permanent are these effects? Could they, for example, occur 15 between inlet characterizations in the field and compromise results?

15 Unfortunately, we can't say for certain what those uncertainties are, or how permanent they are. This is why it is important to discard any ovens with obvious problems, and characterize the ones we do use very well. We have included a line in the discussion which emphasizes this. P20L5 now reads: "Based on the 20 results of this paper, we make the following three recommendations: (1) TD ovens should be characterized with the appropriate reactive nitrogen compounds regularly at the oven set points using the oven residence time and gas pressure that will be used in ambient sampling. This is especially important given the findings of the Berkeley group regarding impurities found in otherwise identical ovens, as discussed in Sect. 3.1."

25 pg 15, line 20. NH_4NO_2 – typo

Thank you for catching this, we have fixed the typo.

pg 18, line 27. Slusher *et al.* 2004 is not a suitable reference as CIMS quantifies PAN and N_2O_5 at different masses and no corrections are necessary.

30 We were trying to say that Slusher *et al* had considered the recombination of $NO_3 + NO_2$ after the heater as a possible interference. However, it is true that this was not clearly stated, so because that paragraph had already been rewritten (see our response to Reviewer #3's comment on page 18, lines 22-23), we simply removed that statement.

35 Figure S7. Not sure what is meant by 0 nm sized particles – maybe it should be "no particles"?

This is indeed confusing. The 0 nm refers to setting the DMA size (and voltage) to 0, to ensure that no particles get through. Of course, it is possible for a few very small particles to get through, which is why we wanted to test the throughput at this voltage setting. We have included a line in the figure caption that 40 explains this more clearly: "Here, "0 nm" refers to setting the DMA voltage to 0, which nominally does not allow any particles through."

Evaluation of the accuracy of thermal dissociation CRDS and LIF techniques for atmospheric measurement of reactive nitrogen species

Caroline C. Womack¹, J. Andrew Neuman^{1,2}, Patrick R. Veres^{1,2}, Scott J. Eilerman^{1,2}, Charles A. Brock¹, Zachary C. J. Decker³, Kyle J. Zarzana^{1,2}, William P. Dube^{1,2}, Robert J. Wild^{1,2}, Paul J. Wooldridge⁴, Ronald C. Cohen^{4,5}, Steven S. Brown^{1,3}

¹Chemical Sciences Division, Earth Science Research Laboratory, National Oceanic and Atmospheric Administration, Boulder, CO 80305 USA

²Cooperative Institute for Research in Environmental Sciences, University of Colorado, Boulder, CO 80309 USA

10 ³Department of Chemistry and Biochemistry, University of Colorado, Boulder, CO 80309 USA

⁴Department of Chemistry, University of California, Berkeley, CA 94720 USA

⁵Department of Earth and Planetary Science, University of California, Berkeley, CA 94720 USA

Correspondence to: S. S. Brown (steven.s.brown@noaa.gov)

Abstract. The sum of all reactive nitrogen species (NO_y) includes NO_x (NO₂ + NO) and all of its oxidized forms, and the accurate detection of NO_y is critical to understanding atmospheric nitrogen chemistry. Thermal dissociation (TD) inlets, which convert NO_y to NO₂ followed by NO₂ detection, are frequently used in conjunction with techniques such as laser induced fluorescence (LIF) and cavity ringdown spectroscopy (CRDS) to measure total NO_y when set at >600 °C, or speciated NO_y when set at intermediate temperatures. We report the conversion efficiency of known amounts of several representative NO_y species to NO₂ in our TD-CRDS instrument, under a variety of experimental conditions. We find that the conversion efficiency of HNO₃ is highly sensitive to the flow rate and the residence time through the TD inlet, as well as the presence of other species that may be present during ambient sampling, such as ozone (O₃). Conversion of HNO₃ at 400 °C, nominally the set point used to selectively convert organic nitrates, can range from 2-6% and may represent an interference in measurement of organic nitrates under some conditions. The conversion efficiency is strongly dependent on the operating characteristics of individual quartz ovens, and should be well calibrated prior to use in field sampling. We demonstrate quantitative conversion of both gas phase N₂O₅ and particulate ammonium nitrate in the TD inlet at 650 °C, the temperature normally used for conversion of HNO₃. N₂O₅ has two thermal dissociation steps, one at low temperature representing dissociation to NO₂ and NO₃, and one at high temperature representing dissociation of NO₃, which produces exclusively NO₂ and not NO. We also find a significant interference from partial conversion (5-10%) of NH₃ to NO at 650 °C in the presence of representative (50 ppbv) levels of O₃ in dry zero air. Although this interference appears to be suppressed when sampling ambient air, we nevertheless recommend regular characterization of this interference using standard additions of NH₃ to TD instruments that convert reactive nitrogen to NO or NO₂.

1 Introduction

The catalytic cycling of nitrogen oxides ($\text{NO}_x = \text{NO} + \text{NO}_2$) plays a key role in the formation of tropospheric ozone (O_3) from the photooxidation of VOCs. Reactive nitrogen species, such as alkyl and multifunctional nitrates (ANs, RONO_2), peroxy nitrates (PNs, RO_2NO_2) and nitric acid (HNO_3) serve as reservoirs and sinks of NO_x . The formation of these species results in chain termination that determines the efficiency of the O_3 production cycle, and can also transport NO_x far from the original emission source. For this reason, total reactive nitrogen ($\text{NO}_y = \text{NO} + \text{NO}_2 + \text{RONO}_2 + \text{RO}_2\text{NO}_2 + \text{HNO}_3 + \text{HONO} + \text{NO}_3 + 2 \times \text{N}_2\text{O}_5 + \text{aerosol nitrates}$) is an important tracer in monitoring tropospheric O_3 production. Its accurate detection is critical in field measurements of ambient air quality, as O_3 is a known health risk, and a number of regions across the US are currently in non-attainment or near non-attainment with national ambient air quality O_3 standards (EPA, 2016). However, the sources and fates of NO_y species are complex and remain poorly characterized in some regions. Measured total reactive nitrogen has in some cases deviated significantly from the sum of the measured individual components, $\Sigma\text{NO}_{y,i}$ (see (Fahey et al., 1986;Bradshaw et al., 1998;Neuman et al., 2012) and others referenced within). This unmeasured NO_y , sometimes referred to as “missing NO_y ”, indicates the need for a more complete understanding of total and speciated reactive nitrogen, and for accurate analytical instrumentation for NO_y measurement (Crosley, 1996;Williams et al., 1998;Day et al., 2003).

Techniques that detect the major individual components of NO_y include detection of NO and NO_2 by chemiluminescence (Ridley and Howlett, 1974;Kley and McFarland, 1980), cavity ringdown spectroscopy (CRDS) (Fuchs et al., 2009), or laser induced fluorescence (Thornton et al., 2000), and detection of HNO_3 by chemical ionization mass spectrometry (CIMS) (Fehsenfeld et al., 1998;Huey et al., 1998;Neuman et al., 2002;Huey, 2007) or mist chamber sampling (Talbot et al., 1990). Additionally, speciated peroxy acetyl nitrates (PANs) have been detected by gas-chromatography electron capture detection (Darley et al., 1963;Flocke et al., 2005) and CIMS (Slusher et al., 2004), while N_2O_5 and ClNO_2 have been detected by CRDS (Dubé et al., 2006;Thaler et al., 2011) and CIMS (Kercher et al., 2009).

HONO has been detected by long path differential optical absorption spectroscopy (Perner and Platt, 1979) and NO_3 has been detected by CRDS (King et al., 2000). However, fewer methods have been developed for detection of the broad suite of individual alkyl and multifunctional nitrates, which have been suggested to comprise upwards of 20% of NO_y in the midlatitude continental boundary layer and may be higher in remote locations (O'Brien et al., 1995;Day et al., 2003;Worton et al., 2008;Beaver et al., 2012;Xiong et al., 2015;Lee et al., 2016). An alternative to detecting individual components of NO_y is the use of a molybdenum oxide or gold catalyst in the presence of CO to reduce all NO_y species to NO , followed by NO detection by chemiluminescence (Winer et al., 1974;Fahey et al., 1986), though catalyst-based techniques are known to require frequent cleaning, and are potentially sensitive to contamination

Formatted: Subscript

Formatted: Highlight

and to interferences at ambient levels of ammonia, HCN, acetonitrile, and R-NO₂ compounds (Crosley, 1996;Kliner et al., 1997;Bradshaw et al., 1998;Williams et al., 1998;Day et al., 2002). An alternative method developed by Day and co-workers (Day et al., 2002) uses a quartz thermal dissociation (TD) inlet to rapidly thermally convert nearly all NO_y species to NO₂, which is then detected by laser induced 5 fluorescence (LIF). The NO_y species in the TD inlet undergo the following reaction



where X is HO, RO, or RO₂. Heated inlets had previously been used to dissociate PNs (Nikitas et al., 10 1997), but the TD inlet developed by Day et al. (2002) takes advantage of the different O-N bond energies of ANs, PNs, and nitric acid to separately and selectively detect these three classes of NO_y. A plot of measured NO₂ signal as a function of inlet temperature (hereafter referred to as a “thermogram”) yields a stepwise dissociation curve with increases in signal near 100, 300 and 500 °C, corresponding to the dissociation of PNs, ANs, and HNO₃ respectively. By setting the TD oven temperature to one of the three 15 plateaus, they were able to measure each class of NO_y, by comparison of the NO₂ signal in a given channel to the signal measured at the adjacent lower temperature plateau.

In recent years, a suite of other instruments have incorporated this NO_y TD inlet method into existing techniques that measure NO₂ or the radical cofragment X in Eq. (1), such as chemical ionization 20 mass spectrometry (TD-CIMS) (Slusher et al., 2004;Zheng et al., 2011;Phillips et al., 2013), cavity ringdown spectroscopy (TD-CRDS) (Paul et al., 2009;Thieser et al., 2016), and cavity attenuated phase shift spectroscopy (TD-CAPS) (Sadanaga et al., 2016). Each instrument has its own advantages and disadvantages. For example, TD-LIF detects NO₂ at low pressure following thermal dissociation, ~~which minimizes secondary recombination reactions of the dissociated radicals~~ would thus be suppressed in the detection region, although the thermal dissociation inlet may be operated at either high or low pressures in these instruments. However, it ~~but~~ is subject to interferences from ~~ambient urban~~ levels of NO and NO₂ 25 (Paul et al., 2009;Wooldridge et al., 2010). TD-CIMS can differentiate between the different types of PNs ~~or ANs~~, but requires regular calibration of each species, not all of which have native standards readily available. TD-CAPS is subject to interferences from glyoxal and methylglyoxal (Sadanaga et al., 2016). TD-CRDS is an absolute measurement, but can be subject to other interferences, as discussed in Sect. 3.

Recent TD inlet studies (Day et al., 2002;Paul et al., 2009;Thieser et al., 2016) have measured the 30 conversion efficiency for several AN and PN species with known concentrations in a laboratory setting. These studies all note the possibility of secondary reactions that either increase or decrease the NO₂ signal. For example, recombination reactions to reform the AN or PN species prior to reaching the detector will result in a negative ~~artifact bias~~ in NO₂ (too little NO₂ measured). Likewise, ambient levels

of O_3 in the sampled air (or the O atoms that form in O_2 -pyrolysis) may react in the oven with NO to form NO_2 , resulting in a positive artifact bias (Pérez et al., 2007), though this reaction rate depends on the TD inlet pressure and flow rate (Wooldridge et al., 2010). Day et al. (2002) found that recombination reactions were significant for PNs, but caused minimal problems for nitric acid, since the OH radical is far more likely to be lost to the walls of the oven than to recombine with NO_2 . More significant is the reaction of dissociated RO_2 and HO_2 radicals with ambient levels of NO and NO_2 . Thieser et al. (2016) parameterized the bias in peroxyacetyl nitrate and 2-propyl nitrate detection in their inlet as a function of ambient NO and NO_2 concentrations, but noted that these parameterizations may vary for other PNs or ANs. ~~These effects are generally considered minor compared to other uncertainties in the measurement,~~ 10 ~~but~~ In cases where the concentration of one category of NO_y species far exceeds the others, such as the high HNO_3 :ANs ratios in Pusede et al. (2016), speciated measurements can be significantly affected by biases in measurements of the other NO_y compounds.

A four-channel CRDS instrument (hereby referred to as the NOAA TD-CRDS instrument) for detection of nitrogen oxides was recently developed (Wild et al., 2014). In this instrument, one channel is equipped with a TD inlet set at 650 °C and is used to measure all NO_y species (including NO_2 , and NO by chemical conversion with an O_3 addition to NO_2). Two other channels simultaneously monitor NO_2 and NO, and so a measurement of NO_z (= $NO_y - NO_x$) can be derived. Because NO is intentionally detected as NO_2 in the NO_y channel, this instrument avoids the majority of the $NO \leftrightarrow NO_2$ interconversion interferences that affect many other thermal dissociation instruments. Analogous to the studies which measured the conversion efficiencies of ANs and PNs (Day et al., 2002; Paul et al., 2009; Sadanaga et al., 2016; Thieser et al., 2016), we present here an analysis of the conversion efficiencies of several other NO_y species, and the interferences that affect the operation of this high temperature inlet. These interferences include the temperature dependence of HNO_3 conversion, which is important to understanding both its quantitative conversion at 650°C as well as its potential to interfere with measurements of ANs at lower temperatures. We also compare these results to those from the TD-LIF instrument of Day et al. (2002), hereby referred to as the Berkeley TD-LIF instrument. Additionally, we report the temperature dependence of N_2O_5 conversion, which is shown to occur in two steps, the conversion efficiency of ammonium nitrate aerosol, and finally the interference of NH_3 through its partial conversion to NO.

2 Methods

30 2.1 Thermal dissociation cavity ringdown spectroscopy (TD-CRDS)

Cavity ringdown spectroscopy is a direct absorption technique for measuring the concentration of trace gases (O'Keefe and Deacon, 1988; Fuchs et al., 2009). The four-channel 405 nm NOAA TD-CRDS

instrument, which has been used by our group in both lab-based studies and atmospheric sampling (Wild et al., 2014; Wild et al., 2016), simultaneously measures ambient NO₂ in one channel, while chemically converting NO and O₃ to NO₂ in the second and third channels, and thermally converting NO_y to NO₂ in a TD oven in the fourth channel. In this study, we have used only the NO_y channel to study the conversion efficiency of several reactive nitrogen species to NO₂. Figure 1 shows a schematic of the relevant instrument plumbing and optical cavity. The details of the optical cavity can be found in (Wild et al., 2014); only a brief description of the optical system and the details of the TD inlet that deviate from that study will be described here.

Sampled air is pulled into a 50 cm long high-finesse optical cavity capped by highly reflective end mirrors, with purge flows of 25 sccm (cubic centimeters per minute at 273.15 K and 1 atm) added in front of each mirror to maintain mirror cleanliness. The output of a 0.5 nm bandwidth, continuous wave diode laser centered at approximately 405 nm and modulated at 2 kHz is passively coupled into one end of the optical cavity. The laser light builds up in the cavity, and when it is modulated off, the decaying output light intensity is monitored by photomultiplier tube on the far side of the cavity. The measured light decay profiles are summed and fit at a 1 Hz repetition rate to yield the ringdown time τ . The ringdown time is inversely related to the concentration of the absorbing gas, NO₂ in this case, which can be derived as

$$[NO_2] = \frac{R_L}{c\sigma} \left(\frac{1}{\tau} - \frac{1}{\tau_0} \right) \quad (2)$$

where R_L is the ratio of d , the mirror separation length, and l , the distance over which the sample is present. The speed of light is represented by c , σ is the absorption cross section of NO₂, and τ_0 is the ringdown time of a reference cavity without any absorbing gases, which is obtained by flushing the cavity with an excess flow of zero air for 30 seconds every 10 to 20 minutes. If purge volumes were not used, the R_L term in Eq. (2) would simply be 1, but since purge volumes are used here, σ/R_L is calibrated characterized regularly by filling the cavity with several different known NO₂ concentrations (obtained by reacting the output of an O₃ standard source with excess NO) and calculating the slope of the measured optical extinction vs [NO₂] as described in Washenfelder et al. (2011). This value was measured approximately once per month during laboratory tests with this instrument, but was constant to within $\pm 1\%$, with an average value of $6.25 \times 10^{-19} \text{ cm}^2$. More regular calibrations of the σ/R_L value during recent field studies show similar stability. The NO₂ signal can be measured with a lower detection of 18 pptv (1σ) in 1 second (Wild et al., 2014).

Formatted: Subscript

The NO_y TD oven inlet consists of a quartz tube (0.39 cm ID, 63 cm in length, 38 cm of which is heated) wrapped in Nichrome wire and insulated with fiberglass. The flow rate through the inlet and optical cavity is controlled by a mass flow controller on the downstream side of the optical cavity. Because the standard flow rate is held constant during each experiment, the volumetric flow rate, and therefore the TD residence time, varies with oven temperature. For example, the 4.5 cm³ inner volume of the oven results in an oven residence time of 30 - 100 ms at a flow rate of 1.9 slpm (slpm = liters per minute at 273.15 K and 1 atm) for temperatures from 25 – 650 °C. 1.9 slpm represents the normal operating conditions of this instrument, but flow rates between 0.25 and 3 slpm were tested, which provides oven residence times between 20 and 400 ms. The temperature of the TD oven is monitored by a thermocouple mounted to the outer side of the quartz tube, and therefore is slightly lower than the temperature of the gas. However, inserting a temperature probe into the inner part of the TD inlet yields a temperature profile, shown in Fig. S1, which approaches the temperature set point by the end of the inlet. All oven temperatures described hereafter refer to the measured thermocouple temperature. After passing through the TD oven, the gas cools to room temperature in the non-heated portion of the quartz tube, passes through a particle filter (47 mm diameter, 1 µm pore size PTFE membrane) to remove non-volatilized particles, and then enters a 15 cm³ mixing volume prior to entering the CRDS cavity. There, O₃ (~30 ppmv after dilution) is added to the sampled air to convert any NO that formed in the thermal dissociation to NO₂. As the rate constant for the NO + O₃ → NO₂ + O₂ reaction is more than three orders of magnitude faster than the NO₂ + O₃ → NO₃ + O₂ reaction, conversion of NO₂ to NO₃ (and subsequently to N₂O₅) is at most 1-2% in this mixing volume and is corrected for using a previously described method (Fuchs et al., 2009). To measure the thermograms shown in this paper, the oven temperature was set to a sequence of temperatures spanning 300 to 650 °C and spaced by 25 °C in a random order. The measured NO₂ concentrations are averaged at each temperature set point for approximately 10 – 15 minutes.

25 2.2 NO_y samples and additions

Samples of reactive nitrogen species (labeled as “NO_y source” in Fig. 1) were introduced into the TD oven in several ways. HNO₃ and NH₃ were obtained by passing a 50 sccm flow of zero air through a calibrated 45 °C permeation tube containing HNO₃ (VICI Metronics) or NH₃ (KinTek), providing gaseous outputs of 64 and 23 ng/min, respectively (Neuman et al., 2003). Subsequent dilution in 0.5 - 4 slpm zero (synthetic) air resulted in HNO₃ and NH₃ concentrations of 5 to 40 ppbv. Because both these species readily adsorb to instrument surfaces (Neuman et al., 1999), only FEP Teflon tubing was used between the permeation tube and the TD oven, all tubing was kept as short as possible (typically less than 30 cm) and was wrapped in 100°C heating tape to reduce losses to the walls. However, these precautions

were found to be unnecessary in this laboratory study, since the constant flow from the permeation tube resulted in an equilibrium in which the adsorption losses to the walls were equal to the rate of off-gassing.

NO was obtained by dilution of the output of a calibrated standard (Scott-Marrin, 0.2% in N₂). N₂O₅ was synthesized via a procedure adapted from Davidson et al. (1978) and Bertram et al. (2009), which has been used as a calibration for the N₂O₅ channel of a CRDS NO₃ instrument (Dubé et al., 2006; Wagner et al., 2011). Pure samples of NO and O₂ were mixed to yield NO₂, and this mixture was reacted in a flow tube with excess O₃, yielding NO₃ which then reacted with NO₂ to form N₂O₅. The resulting mixture flowed through a glass trap at -78°C, where N₂O₅ solidified as a white crystal. A gaseous sample of N₂O₅ was obtained by flowing 20 - 50 sccm of zero air over the solid -78 °C sample, and then diluting further in zero air. Gas phase N₂O₅ prepared in this way is known to contain variable but significant amounts of HNO₃ (Bertram et al., 2009), and thus efforts were made to minimize this interference by baking all glassware for several hours before use, and by distilling the solid N₂O₅ sample regularly by bringing it to room temperature under an O₃ flow for 10 minutes. Nevertheless, some HNO₃ was always present in the sample, and therefore the output of the trap was passed through a nylon wool scrubber prior to entering the TD oven, which removed HNO₃ without significantly perturbing the N₂O₅ concentration. Finally, ammonium nitrate particles were generated by running a 0.1 g/L solution of aqueous NH₄NO₃ through an atomizer and size-selecting particles of a certain diameter with a custom-built differential mobility analyzer (DMA). Conductive tubing, rather than Teflon, was used to minimize electrostatic build up and loss of particles to the walls before entering the TD oven.

In order to test whether common atmospheric gases would interfere with the conversion efficiency, some additional species were added to the sample prior to entering the oven. Water was added by bubbling-passing the dilution zero air through a water bubbler prior to mixing with the HNO₃ sample. Various amounts of O₃ were added by running the dilution zero air through an O₃ calibrator (Thermo Scientific 49i) that is also capable of generating up to 200 ppm O₃ in 1 - 3 slpm of zero air. We also investigated the effect of various VOCs, including a high concentration of propane (~5 ppmv) and a standard mixture of VOCs (Air Liquide) consisting of n-hexane (1.234 ppm), propanal (0.397 ppm), 2-butanone (1.237), benzene (1.151 ppm), methylcyclohexane (0.938 ppm), ethylbenzene (1.213 ppm), 2,2,4-trimethylpentane (1.186 ppm), isopropyl benzene (1.148 ppm) and ethanol (0.994 ppm). This mixture is commonly used to calibrate GC/MS instruments, but here provides common atmospheric species with a range of masses, bond strengths, and degrees of oxidation. It was diluted to 50 ppbv total VOCs by addition of zero air prior to entering the oven. We also added CO in varying quantities to the HNO₃ and NH₃ samples.

2.3 Ancillary measurements

Several instruments were used as ancillary confirmation for some of the NO_y sample concentrations. In each case, a Teflon tee split the sample input and a portion of the flow was pulled into the secondary instrument prior to entering the TD oven, as shown in Fig. 1. In the case of NH₃, a Picarro G2103 NH₃ Analyzer with a manufacturer's specified 1 ppbv detection limit at 5 second integration time was used. A custom-built iodide adduct chemical ionization mass spectrometer (Lee et al., 2014), described in further detail in (Veres et al., 2015), was used to monitor the N₂O₅ and HNO₃ concentrations from the N₂O₅ solid sample prior to dissociation in the oven. In this instrument, N₂O₅ and HNO₃ mixed with I⁻ ions produced by passing CH₃I through a ²¹⁰Po source, and the resulting HNO₃·I⁻ and N₂O₅·I⁻ ions were detected by quadrupole mass spectrometry at m/z = 190 and 235 respectively. This measurement has a detection limit of 4 pptv and 70 pptv and error bars of 25% and 25% (3 σ) for N₂O₅ and HNO₃ respectively. Lastly, an ultra-high sensitivity aerosol spectrometer (Droplet Measurement Technologies) was used to monitor the size distribution of the size-selected ammonium nitrate particles (Cai et al., 2008).

HNO₃ and NH₃ conversion efficiencies were also tested using ambient air for dilution (rather than synthetic air), as sampled during daytime in August 2016 in Boulder, CO. Ambient air was drawn into the two of the four channels of the NOAA TD-CRDS instrument, through two side-by-side identical quartz ovens heated to 650 °C at a flow rate of 1.4 slpm, and the output of either the NH₃ or HNO₃ permeation tube was inserted directly into the exposed inlet of one of the ovens, for a duration of approximately 6 minutes. The NO₂ signal was measured by one of the remaining channels in the NOAA TD-CRDS instrument, and the conversion efficiency of each species was calculated by comparing the difference in NO₂ signal between the two ovens relative to the calibrated output of the permeation tube, to correct for small differences in NO₂ signal between the two ovens.

We also present results measured in the Berkeley TD-LIF instrument. It is described in greater detail elsewhere (Day et al., 2002), but briefly, HNO₃ and *n*-propyl-nitrate samples were provided by permeation tubes similar to those described in Sect. 2.2, diluted in dry zero air, and passed through 20 cm heated length quartz ovens, held at ambient pressure, at a flow rate of 2 slpm. This resulted in residence times of approximately 50 ms. The NO₂ released in the thermal conversion was supersonically expanded into the detection region and measured by laser induced fluorescence from an individual ro-vibronic NO₂ line. The NO_y conversion ratio was calculated as the measured NO₂ concentration relative to the maximum NO₂ signal at high temperatures, as the oven temperature was changed at a rate of -10 °C per minute.

Formatted: Subscript

Formatted: Subscript

Formatted: Subscript

2.4 Box modeling

A simple kinetic box model was used to support the experimental findings. [Rate laws](#)[Reaction rates](#) for ~60 reactions possibly involved in the dissociation and secondary chemical reactions of each NO_y species (listed in the Supporting Information), were obtained from the JPL Kinetics Database (Sander et al., 2011) and the NIST Chemical Kinetics Database (Manion et al., 2015) at temperatures spanning the 25 - 650 °C range of the experimental thermograms. For every HNO₃, N₂O₅, and NH₃ thermogram, a simulation was run at each temperature, assuming a starting concentration of the NO_y species equal to that observed in the experiment, and lasting the duration of the residence time in the oven. The simulation was then allowed to keep running at room temperature for an additional ~1 second to mimic the conditions between the oven and the instrument. During this additional low temperature time, 30 ppmv of O₃ was added to the simulation to convert NO to NO₂ as in the TD-CRDS instrument. The final concentration of NO₂ at the end of the simulation was recorded for each temperature, which resulted in a simulated thermogram. Several simplifying assumptions were made here. We assume instantaneous heating and cooling of the sample, and a uniform temperature profile along the 38 cm length of the TD oven. We also only consider gas-phase reactions, and neglect any surface-mediated reactions. When possible, JPL-recommended values for the rate constants were used, but many of those listed did not span the full temperature range of the thermograms. When JPL values were not available, [rate laws](#)[reaction rates](#) from the NIST database were used (see Table S1). We also derive temperature-dependent wall loss constants for O and OH using the procedure outlined by Thieser et al. (2016), but find that better agreement in some simulations can be achieved with the experimental data by using an empirical value, or no wall loss at all. As can be seen in Sect. 3, these simulations successfully replicated a major portion, but not all, of the experimental results, likely due to these simplifications.

3 Results

3.1 HNO₃ thermograms

Formatted: Subscript

Figure 2 shows the conversion efficiency of HNO₃ to NO₂ as a function of temperature, for several flow rates through the ~~oven~~[NOAA TD-CRDS](#). Conversion efficiency was calculated as the measured NO₂ mixing ratio divided by the input HNO₃ mixing ratio. The box model simulations for each flow rate are shown as solid lines of corresponding color. The HNO₃ permeation tube has a calibrated output of 64 ng/min, which corresponds to an expected HNO₃ concentration of between 5 and 40 ppbv, depending on the zero air dilution required for each flow rate. The output of the permeation tube was found to contain approximately 2.5% NO₂ and all HNO₃ thermograms have had this 2.5% baseline signal subtracted. At a flow rate of 1.9 slpm (where the oven residence time is 30 - 100 ms depending on temperature), we

observe 100% conversion of HNO_3 at oven temperatures above 600 °C, whereas the thermograms obtained at 1 slpm and 3 slpm reach a maximum conversion of 100% at 550 and 650 °C respectively. The 0.5 slpm thermogram has a slightly lower maximum conversion efficiency (95%), possibly due to the recombination reactions of OH and NO_2 during the extended time in the cool down region prior to detection.

Formatted: Subscript

The box model simulations in Fig. 2 mimic the shape of the experimental data, but some are slightly shifted to higher or lower temperatures, likely because the simulation is extremely sensitive to the flow rate and may be affected by the simplifying assumptions detailed in Sect. 2.4. The shape of the simulated thermogram is entirely controlled by the reaction rate law of the initial dissociation reaction of HNO_3 to $\text{NO}_2 + \text{OH}$. This reaction has a third order rate constant of $k_0(T) = 1.82 \times 10^{-4} \cdot (T/298)^{1.98} \cdot e^{(-24004/T)}$ and a high-pressure limit of $k_\infty(T) = 2 \times 10^{15} \cdot e^{(-24054/T)}$ (Glänzer and Troe, 1974) and thus at a midrange temperature such as 500 °C, the HNO_3 lifetime is approximately 250 ms. The inner volume of the oven is 4.5 cm³, and so at a flow rate of 1.9 slpm, the gas has a plug flow residence time of 38 ms in the 500 °C oven, compared to a residence time of 77 ms at 1.0 slpm and 153 ms at 0.5 slpm. The simulated conversion efficiency in these mid-range temperatures is therefore extremely sensitive to the flow rate, in agreement with our experimental results. However, the experimental 100% conversion efficiency at high temperatures indicates that there is virtually no recombination of OH and NO_2 once formed, because the recombination rate for $\text{OH} + \text{NO}_2$ is quite low, and because OH radicals are far more likely to be lost to the walls of the oven (at a diffusion-limited rate determined by Day et al. (2002) of ~46 s⁻¹ for 1/4" OD tubing, which is far higher than the pseudo-first order recombination rate coefficient of 0.075 s⁻¹ at $[\text{NO}_2] = 10 \text{ ppbv}$). No attempt was made to dilute the output of the HNO_3 permeation tube any further, as recombination effects would likely only be less important at lower starting HNO_3 concentrations. Similarly, increasing the starting NO_2 concentration, to mimic conditions in highly polluted environments, was not attempted in this set of experiments, but increasing the starting NO_2 concentration in the kinetic model up to 50 ppbv shows that there is no recombination expected even with elevated NO_2 in the oven. This is in contrast to ANs and PN, for which the reaction of the dissociated peroxy and alkyl radicals with NO_2 is a significant interference (Thieser et al., 2016), but in good agreement with the HNO_3 results of Day et al. (2002) and Sobanski et al. (2016).

Formatted: Superscript

Formatted: Subscript

Formatted: Subscript

Formatted: Subscript

Formatted: Subscript

Formatted: Subscript

Formatted: Subscript

At a flow rate of 1.9 slpm, we observe a ~6% conversion of HNO_3 to NO_2 at an oven temperature of 400 °C. Although this efficiency is specific to the conditions of the oven used here, it is a key finding since 400 °C is in the vicinity of the temperature set point chosen for selective detection of total alkyl and multifunctional nitrates by TD-LIF (Day et al., 2002) and other TD instruments. This result is in good agreement with Thieser et al. (2016), who found a ~10% HNO_3 conversion at 450 °C. Sadanaga et al. (2016) report ~15% HNO_3 conversion at 360 °C at a TD residence time of 3.4 sec, which exceeds the

range of our study but follows the trend in Fig. 3. In a previous study (Wild et al., 2014), we presented thermograms designed to demonstrate quantitative conversion efficiency at high temperatures. The temperature dependence of thermal conversion was not well constrained at lower temperatures, and showed, for example, 30% conversion at 400 °C. As discussed by Sobanski et al. (2016), the large conversion efficiency presented by Wild et al. (2014) at this temperature is likely incorrect. The extent of HNO_3 conversion is dependent on the residence time in the oven, but because residence time for a given flow rate changes with oven temperature, it is easier to observe this effect by plotting conversion efficiency versus residence time, as in Fig. 3, for five different temperatures (350, 400, 450, 500, and 600 °C). This plot represents transects through Fig. 2 at these five temperatures. Figure S2 shows a log scale plot to highlight the low conversion efficiency region. Most instruments utilizing the TD oven technique use a set point between 350 and 450 degrees and a residence time between 30 and 100 ms to selectively detect ANs and not HNO_3 (Day et al., 2003; Paul et al., 2009; Thieser et al., 2016), but Fig. 3 demonstrates that there is significant variability in the HNO_3 conversion efficiency that depends nonlinearly on oven residence time.

We further measure the effect of pressure on the conversion by placing a heated stainless steel needle valve in front of the oven, thus lowering the pressure inside the oven to 250 mbar. The low pressure transects for each of the five temperatures can be seen in open circles in Fig. 3, and the full thermograms are displayed in Fig. S3. The low pressure transects are slightly lower than those at ambient pressure for the 450 and 500 °C setpoints, but match reasonably well at low and high temperatures, indicating that the onset and final conversion of HNO_3 are not strongly sensitive to pressure. To ensure that HNO_3 was not lost on the walls of the stainless steel valve, the conversion efficiency was measured with the valve fully open, and was found to match that taken with no valve. These experiments demonstrate the importance of verifying that a given temperature set point and flow rate is suitable for measurement of alkyl nitrates without interference from HNO_3 conversion.

To demonstrate the variability within individual TD ovens, an example of the HNO_3 conversion efficiency near the alkyl nitrate temperature setpoint, as measured by the Berkeley TD-LIF instrument, is shown in Fig. 4. This inlet's alkyl nitrate setpoint temperature was chosen to be just past the plateau in the n-propyl-nitrate signal at 410 °C. The HNO_3 conversion to NO_2 was found to be 2.5%, which for most TD-LIF experiments would be negligible compared to other uncertainties in measured ANs ($\pm 15\%$) and no correction ~~was~~^{would} be applied. One example where a correction was significant was for the NASA DISCOVER-AQ California deployment, which took place in California's central valley during a period of high NH_4NO_3 aerosol loading. Ratios of $(\text{HNO}_3 + \text{NH}_4\text{NO}_3)$ to ANs were high enough that a correction was necessary and applied to both observations (Pusede et al., 2016). As HNO_3 is derived by subtraction of the ANs, any HNO_3 conversion at the AN temperature results in a high bias for ANs and an equal low

Formatted: Subscript

Formatted: Subscript

bias for HNO_3 . The sum of the two remains correct independent of the onset of the HNO_3 conversion. The Berkeley group has found the HNO_3 conversion to be oven dependent even for identical pressure and flow conditions indicating some but not all ovens have impurities at the walls that effectively catalyze HNO_3 decomposition. Ovens with high HNO_3 conversion efficiencies at low temperatures were 5 discarded. These results highlight the importance of careful evaluation and calibration of each TD oven, even when the inner volumes and flow rates are similar.

3.2 HNO_3 thermograms with additions

Tests for other interferences to HNO_3 and AN measurements included adding several different chemical species to the HNO_3 sample prior to entering the oven. These were designed to test the 10 hypothesis that certain trace gases found in ambient air would interact with radicals in the oven, or would themselves dissociate to form radicals which could react with NO , NO_2 , OH , or HNO_3 . The results are 15 shown in Fig. 5. In Fig. 5a, a portion of the dilution air was passed through a distilled water bubbler prior to diluting the HNO_3 , bringing the relative humidity up to 66%. The change in RH does not alter the shape, onset, or total conversion efficiency of the thermogram. This is to be expected, as the oven 20 temperature is not high enough to dissociate H_2O to $\text{OH} + \text{H}$, and reactions between H_2O and the relevant species formed in the oven from HNO_3 dissociation are far too slow to be important here. However, it should be noted that both H_2O and HNO_3 are sampled in this experiment at a steady concentration, and it is possible that during ambient sampling, rapid changes in the RH or HNO_3 concentration could change 25 the overall efficiency. Additionally, we did not test the conversion efficiency at very high RH levels, and it's possible there could be a non-linear effect of water. Figure 5b shows the measured thermogram with the addition of ~50 ppbv VOCs (described in Sect. 2.2) with and without the addition of 90 ppbv O_3 , as well as the addition of 5 ppmv of propane, to mimic conditions found in highly polluted wintertime atmospheres. If organic radicals were produced thermally in the TD oven, they could potentially react 30 with NO_2 , thus altering that signal. However, the bond dissociation energy of the C-H or C-C bonds most likely to thermally dissociate in each of the VOCs are all significantly higher (typically >100 kcal/mol) than that of the O-N bond in HNO_3 (~50 kcal/mol) making it unlikely that organic radicals are formed inside the oven from dissociation of VOCs. Reactions of unsaturated hydrocarbons with O atoms or OH radicals tend to be rapid and would produce organic radicals, but these tend to be unstable, and any stable radicals would likely only react with NO_2 to form ANs or PNs. The oven is set at sufficiently high temperatures to dissociate ANs and PNs back to $\text{NO}_2 +$ the organic radical. Addition of these VOCs does not affect the measured conversion efficiency, even in the presence of ambient levels of O_3 . Ozonolysis of the unsaturated hydrocarbons is slow enough (typically on the order of $1 \times 10^{-17} \text{ cm}^3 \text{ molecule}^{-1} \text{ s}^{-1}$) to not have any effect here (we would expect $< 0.0001\%$ reaction for the duration of the oven residence time).

An extremely high concentration of propane also has no effect on the overall conversion efficiency, within the error bars of the measurement, for the same reasons as detailed above.

Figure 5c shows the addition of both small and large quantities of O₃ to the HNO₃ sample. Small quantities do not change the onset or overall conversion efficiency, but larger amounts of O₃ reduce the conversion efficiency at high temperatures. The kinetic box model does not predict this reduction, as it predicts 100% conversion efficiency to NO₂ at all O₃ levels. The dominant bimolecular reaction of O₃ in the model is the reaction with NO₂ to make NO₃, but since this-these reactions isare occurring at high temperature, any NO₃ formed will immediately dissociate to NO₂ (see Sect. 3.2). O₃ also thermally dissociates to O + O₂ at temperatures above 200 °C (see Fig. S4), but the dominant fate of the O radicals should be loss to the walls. Of the O atoms that are not lost to the walls, their primary reaction is also with NO₂ to form either NO + O₂ or NO₃, but NO should be converted back to NO₂ after the oven. Nevertheless, there is an apparent reduction in the conversion of HNO₃ to NO₂ with increasing O₃. While the O₃ concentration range in Fig. 5c exceeds that found in ambient air, highly polluted areas may have large enough O₃ concentrations to make this reduction in conversion efficiency significant. Finally, the addition of 400 ppmv CO in Fig. 5d has a marked effect on the onset, shape, and final conversion of the HNO₃. This addition was tested because gold catalytic NO_y converters require a 1% CO addition to drive the dissociation forward. We find that ~0.5% CO is sufficient to promote HNO₃ dissociation even in the absence of a gold catalyst. However, our kinetic model does not replicate the results of the CO addition. Since the rate-limiting step in these thermograms is the initial dissociation of HNO₃, it is unlikely that the reaction between CO and OH or NO₂ plays a role here. It must therefore be caused by a reaction which changes the rate kinetics of the initial dissociation step. However, to our knowledge there have been no laboratory kinetics studies on the CO + HNO₃ reaction. It is possible-likely that there is some surface reaction that affects the HNO₃ conversion in the presence of CO.

We also note that previous work on TD ovens (Day et al., 2002; Thieser et al., 2016) has cautioned that the elevated temperature of the oven may accelerate the reaction between ambient levels of NO and O₃ to generate NO₂, thereby creating NO₂ signal that is in fact due to ambient levels of NO. This issue does not affect the TD-CRDS NO_y detection scheme, as excess O₃ is intentionally added to the mixing volume after the oven to convert NO to NO₂ to measure total NO_y. Nevertheless, we have investigated how NO responds in the oven, and the results are shown in Fig. S5. A 15 ppbv NO sample was passed through the oven. When no excess O₃ is added to the mixing volume, no NO₂ signal is seen, and when mixing volume O₃ is added, full conversion of NO to NO₂ is observed, as expected. However, when 100 ppbv of O₃ is added to the oven (with no mixing volume O₃ addition), approximately 2.2 ppbv NO₂ signal was observed, or a 15% conversion. This is consistent with the kinetic rate laws-expressions

Formatted: Subscript

Formatted: Not Superscript/ Subscript

Formatted: Subscript

for $\text{NO} + \text{O}_3$ and $\text{NO} + \text{O}$, but we do not differentiate between these two mechanisms in these experiments, as O_3 will always form O at the elevated oven temperatures.

3.2 N_2O_5 thermograms

Figure 6 shows the measured thermogram of N_2O_5 [in the NOAA TD-CRDS](#) at ambient pressure and flow rates of 1.9 and 1.0 slpm, with the kinetic model simulations for each flow rate shown in solid and dashed lines. Two distinct dissociation steps are observed and confirmed by the kinetic model, one between 30 and 110 °C corresponding to the dissociation of N_2O_5 to $\text{NO}_2 + \text{NO}_3$, and one above 300 °C corresponding to the dissociation of NO_3 . The N_2O_5 synthesis method also produces HNO_3 (Bertram et al., 2009) and because the bond enthalpies of NO_3 and HNO_3 dissociation are similar (both ~50 kcal/mol), the thermograms of these two species are expected to overlap at high temperatures. Thus a nylon wool scrubber was used to remove HNO_3 , and the scrubbed sample was simultaneously monitored with an iodide chemical ionization mass spectrometer, described in Sect. 2.3, to ensure the HNO_3 (and not the N_2O_5) was completely removed. The flow rate was lowered to 1.0 slpm in the high temperature scans to accommodate both instruments with better signal-to-noise. The CIMS measured approximately 120 pptv HNO_3 , possibly due to hydrolysis of N_2O_5 after the scrubber, and thus more than 99.5% of the NO_2 signal we observe is attributed to N_2O_5 .

At high temperatures, each N_2O_5 is expected to produce two NO_2 molecules. Conversion efficiency is calculated from the measured NO_2 concentration relative to the N_2O_5 concentration measured by the CIMS instrument, which samples prior to the TD oven. However, the CIMS instrument requires an empirical calibration factor for any species it measures, and while the HNO_3 signal may be calibrated using the permeation tube described in Sect. 3.1, there was no independent calibration available for N_2O_5 – only the signal measured using the TD-CRDS instrument. Therefore, the CIMS N_2O_5 signal was assumed to correspond to a 200% conversion efficiency in the TD-CRDS at 650 °C, and the relative conversion was measured at lower temperatures. The first dissociation step of N_2O_5 to NO_2 and NO_3 is expected at oven temperatures above 110 °C, but because the sample must then travel through a “cool down” region prior to entering the CRDS optical cavity (see Fig. 1), approximately 10% of the NO_2 and NO_3 is expected to recombine back to N_2O_5 , based on the rate constant and the residence time in the mixing volume. This behavior has been well characterized previously (Fuchs et al., 2009) and is accounted for in the data analysis, and as expected, we observe a 91% conversion efficiency of N_2O_5 to NO_2 between 110 and 300 °C. At higher temperatures, NO_3 dissociates in the oven before recombining with NO_2 , and thus a 200% conversion efficiency is observed. While this is not an absolute measure of conversion efficiency, the relative conversion efficiency is consistent with N_2O_5 dissociation and recombination reaction rates to generate two NO_2 molecules in a distinct stepwise manner. At 150 °C and

400 °C, the temperature setpoints often used for detection of PANs and ANs, we find 90% and 105% conversion of N₂O₅ to NO₂, respectively. The exact values are highly dependent on the residence time in both the oven and in the cool down region, but serve to highlight the importance of characterizing the N₂O₅ response in every thermal dissociation oven.

We also measured the conversion of N₂O₅ without the mixing volume O₃ addition at two relevant temperatures, in order to determine the mechanism for NO₃ dissociation. These data are shown in green triangles in Fig. 6, and show no difference in onset or maximum conversion efficiency whether or not mixing volume O₃ is added. As the mixing volume O₃ converts ambient or thermally produced NO to NO₂, the similarity of the two spectra indicates that the NO₃ dissociation mechanism must be NO₃ → NO₂ + O. However, there are no published rate ~~laws-expressions~~ for this reaction and the few studies on NO₃ thermal dissociation have disagreed about whether the reaction proceeds to NO + O₂ (Johnston et al., 1986) or NO₂ + O (Schott and Davidson, 1958). The former argued for the NO₃ → NO + O₂ mechanism based on thermodynamics, as this reaction is exothermic. However, this implies that NO₃ would be thermally unstable at room temperature, which is not the case. It is likely that there is a significant energy barrier to this reaction. The bond enthalpy of the NO₃ → NO₂ + O reaction, on the other hand, is 50.4 kcal/mol, nearly identical to that of HNO₃ → NO₂ + OH, and the two thermograms are very similar in shape and are centered at the same temperature (500 °C). The simulation shown in Fig. 6 is a fit rate ~~law-expression~~ of $k(T) = 1 \times 10^{-2} \cdot (T/298)^0 \cdot \exp(-1500/T)$ obtained by taking the rate ~~law-expression~~ of HNO₃ dissociation and iteratively adjusting it until it matched the data. Essentially identical results were observed in the TD-LIF instrument. (Cohen, 2016).

3.3 NH₄NO₃ thermograms

NH₄NO₃ particles were generated in situ from an aqueous solution, dried, and size-selected by a differential mobility analyzer (DMA) set at 250 nm prior to entering the TD oven. The conversion efficiency was calculated by comparing the measured NO₂ concentration in the TD-CRDS instrument to the expected number of NH₄NO₃ molecules in the aerosol particles, derived from the number and size of the aerosol particles as measured with an ultra-high sensitivity aerosol spectrometer (UHSAS). The measured UHSAS histogram was used, along with the literature value for the density of NH₄NO₃, to convert particle diameter to particle volume, and then to the total number of NH₄NO₃ molecules. We demonstrate here that the dissociation pathway is NH₄NO₃ → NH₃ + HNO₃, and we assume that NH₃ is not converted in any significant fraction. A temperature-dependent baseline NO₂ signal is observed when the DMA voltage is set to zero (i.e. when no particles are transmitted) which is attributed to gas-phase HNO₃ molecules which have evaporated from the particles and adsorbed to the tubing walls, and which are subtracted from the total signal. Figure 7 shows the measured thermogram of NH₄NO₃ with the

thermogram of gas phase HNO_3 from Fig. 2 overlaid. The close agreement between the two thermograms demonstrates that the dissociation pathway is $\text{NH}_4\text{NO}_3 \rightarrow \text{NH}_3 + \text{HNO}_3$, and that this reaction is rapid at the temperatures reached in the TD inlet.

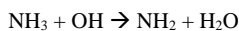
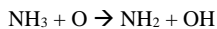
For particles that pass through the DMA at a given size setpoint, the UHSAS measures a size histogram that peaks at a diameter approximately 8% lower, likely because the NH_4NO_3 particles are slightly non-spherical, and therefore the electrical mobility diameter is slightly larger than the geometric diameter. This phenomenon has been discussed at length elsewhere (DeCarlo et al., 2004), and we make no attempt to further characterize NH_4NO_3 particle behavior in the DMA – we have simply taken the UHSAS histogram data to calculate the particle volume, even though this is also subject to slight differences based on the refractive index of NH_4NO_3 . However, if the TD oven failed to volatilize and convert all NH_4NO_3 particles to HNO_3 and then to NO_2 , the measured thermogram would deviate from the HNO_3 spectrum at lower temperatures, where perhaps the heat is not sufficient to drive the NH_4NO_3 out of the condensed phase. The close match between the two is a good indication that the conversion goes to completion. Additionally, Figs. S6 and S7 show a sample NO_2 measurement measured by TD-CRDS at 650 °C as the particle diameter setpoint is changed. There is no correlation between particle size and conversion efficiency, indicating that the oven is completely converting all particles without a size dependence.

3.4 NH_3 thermograms

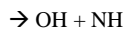
A previous study (Wild et al., 2014), investigated whether ambient levels of ammonia would represent an interference to NO_y conversion, and found that it made at most a 1% difference to the NO_2 signal in dry air, but that this effect was suppressed when $\text{RH} > 10\%$. We find in the present study that there is a significant interference when ambient levels of both NH_3 and O_3 are present in the oven, but that this effect is potentially suppressed by other species found in ambient sampling. Figure 8 shows a thermogram of NH_3 with and without 100 ppbv O_3 present in the oven. The conversion of NH_3 to NO_2 at 650 °C, calculated as the observed NO_2 signal relative to the added NH_3 concentration, is small without O_3 . This is consistent with the previous study of Wild et al. (2014). However, when 100 ppbv of O_3 is added, the thermogram reaches a maximum molar conversion efficiency of 8%, with an onset near 400 °C (red circles). In contrast to the HNO_3 thermograms, however, this signal does not appear to plateau at 650 °C but rather continues to grow at higher temperatures. This result is similar to the interference reported by Dillon et al. (2002), which was attributed to a reaction between NH_3 and O_3 . The interference is only present when O_3 is added to the mixing volume, indicating that the conversion of NH_3 must be producing NO , rather than NO_2 , and is subsequently unimportant to instruments that measure NO_2 only, such as the Berkeley TD-LIF instruments. A kinetic model simulation of both experiments is shown in solid line in

Fig. 8. This simulation was carried out with 35 relevant reactions between NH_3 , O_3 , and the radicals that are formed from these two species in the oven, with the most important reactions are listed below. The reaction between NH_3 and O_3 is far too slow to be relevant here, and the oven temperature is not high enough to dissociate NH_3 to $\text{NH}_2 + \text{H}$ ($\Delta H = 108 \text{ kcal/mol}$). However, O_3 dissociates readily at oven

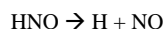
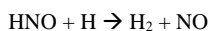
5 temperatures above 200 °C, and once formed, the O atoms may react with NH_3 to form NH_2 .



The reactions of NH_3 are the slowest steps, but once formed, NH_2 reacts readily with O atoms.



HNO then reacts with O, OH, and H to form NO, or can also directly dissociate to form H + NO.



The OH and H atoms formed in Eq. (4) and (5) then drive Eq. (3) further. This mechanism takes place

entirely in the gas phase, and does not take into account any surface-mediated reactions. Many of these reactions have only limited published studies, so the simulation used rate constants that have not been

20 extensively tested. Additionally, to achieve a significant conversion of NH_3 to NO, it was necessary to decrease the O and OH wall loss constants in the model. ~~However, even if~~ This rudimentary simulation

predicts the initial signal increase starting at 300 °C, though general shape of the experimental data, ~~although~~ it has a maximum conversion efficiency of just under 2%, which is below that observed in the

25 experiment. In Fig. 9, we adjusted the amount of added O_3 , while monitoring the conversion efficiency of

NH_3 to NO_2 at an inlet temperature of 650 °C. We find that increasing the O_3 increases the conversion,

which is consistent with $\text{NH}_3 + \text{O}$ being the limiting reaction to make NH_2 . Figure 9 also demonstrates

30 that the conversion of NH_3 is partially quenched by the addition of ambient levels (~100 ppbv) of CO,

likely because the $\text{CO} + \text{O} \rightarrow \text{CO}_2$ reaction competes with those in Eq. (3). Figure 10 shows that the

average conversion efficiency of NH_3 when measured in ambient air in Boulder, CO in August 2016

(which contains 40-60 ppbv O_3 , >80 ppbv CO, ~15% RH, and other species) is $0.5 \pm 2.4\%$, or zero to

within the 1σ error from repeated measurements. This is in contrast to the conversion efficiency of HNO_3

in ambient air, shown in the upper right frame of Fig. 10, which is largely unchanged from that measured

in zero air. Thus, constituents present in ambient air, such as methane, CO, and water, are possibly suppressing the conversion of NH₃ to NO, likely through the reaction with O atoms.

4 Discussion

Using a thermal-dissociation cavity ringdown spectrometer (TD-CRDS), we have quantitatively added reactive nitrogen species to the TD inlet, in order to test the efficiency of the thermal conversion of each species to NO₂, and the effect of any interferences from other trace gases which may be present in the ambient troposphere. We have determined that the TD-CRDS converts HNO₃, N₂O₅, and NH₄NO₃ particles to NO₂ with 100% efficiency at temperatures above 600 °C, but that the onsets of the dissociation are highly dependent on oven residence time. Despite their similar residence times, the NOAA TD-CRDS and Berkeley TD-LIF instruments measure HNO₃ conversion efficiencies ranging from 2.5% to ~8% at 410 °C. It is therefore important that the oven residence time is well characterized in instruments designed to selectively detect ANs without interference from HNO₃. Even two TD ovens with identical inner volumes may exhibit different response functions if they have different ratios of surface area to volume.

We find that high levels of ambient O₃ (>500 ppbv) and CO (>400 ppmv) significantly changed the final conversion efficiency and the onset of the conversion, respectively, of the HNO₃ thermogram, but that ambient levels of a group of representative VOCs and high RH did not affect the measured thermogram. Modest levels of O₃ converted a portion of NH₃ to NO₂. The conversion mechanism likely arises from a gas-phase reaction between oxygen atoms and NH₃ which produces NO. To our knowledge, the NH₃ + O₃ reaction in TD ovens has not been studied in detail, but previous studies of NH₃ conversion in catalytic converters have noted similar results to those presented here – water and CO suppress the NH₃ conversion to NO, while O₃ enhances it (Fahey et al., 1985; Kliner et al., 1997). If not quenched by other species present in ambient air, this effect could represent a potentially significant interference in field sampling for instruments that are sensitive to NO directly, or via conversion to NO₂. For example, at 50 ppbv O₃, the 6% conversion of NH₃ would present an interference of more than 10% if NH₃/NO_y > 1.7, which is not an uncommon condition in agricultural regions. This signal was suppressed in ambient air, indicating that NH₃ may not interfere with NO_y under most conditions. However, ambient air in Boulder is not representative of all sampling conditions, and since the species responsible for quenching the reaction remains unclear, more work must be done to better understand the mechanism of the NH₃/O₃ thermal reaction. This result, along with the others detailed above, serve to emphasize that great care must be taken to characterize the potential interferences in TD NO_y-conversion ovens.

The measured N_2O_5 thermogram exhibits a double dissociation curve, corresponding to the initial dissociation of N_2O_5 to NO_2 and NO_3 , and the subsequent dissociation of NO_3 . Our results indicate that the mechanism of the second step is $\text{NO}_3 \rightarrow \text{NO}_2 + \text{O}$, in contrast to earlier literature that reported $\text{NO}_3 \rightarrow \text{NO} + \text{O}_2$ as the dominant mechanism. To our knowledge, this is the first published thermogram of NO_3 .

5 ~~TD- NO_2 instruments often operate in the daytime when N_2O_5 is not a significant fraction of NO_x , though some groups have operated at night and have typically assumed complete conversion to $\text{NO}_2 + \text{NO}_3$ at the TD inlet setpoint for PNs (Di Carlo et al., 2013), and complete conversion to $2\text{NO}_2 + \text{O}$ at the setpoint for HNO_3 (Wild et al., 2014). These results confirm that there is approximately quantitative conversion at these setpoints, though there are slight deviations from 100% conversion near the PN setpoint. Therefore,~~

10 ~~care must be taken to select a setpoint carefully and ensure complete conversion at that temperature. However, this interference would only be significant during nighttime or during very cold weather sampling. N_2O_5 is not typically considered in the TD NO_2 instrument literature because the existing instruments have largely operated in the daytime, when concentrations of N_2O_5 are not a significant fraction of NO_x . The first dissociation is approximately quantitative at the oven set temperatures used to quantify PN, with the second dissociation occurring at temperatures used for HNO_3 detection. However, this interference would only be significant during nighttime or during very cold weather sampling and is already accounted for in the analysis of these instruments. (Slusher et al., 2004; Thieser et al., 2016)~~

15 ~~TD- NO_2 instruments often operate in the daytime when N_2O_5 is not a significant fraction of NO_x , though some groups have operated at night and have typically assumed complete conversion to $\text{NO}_2 + \text{NO}_3$ at the TD inlet setpoint for PNs (Di Carlo et al., 2013), and complete conversion to $2\text{NO}_2 + \text{O}$ at the setpoint for HNO_3 (Wild et al., 2014). These results confirm that there is approximately quantitative conversion at these setpoints, though there are slight deviations from 100% conversion near the PN setpoint. Therefore, care must be taken to select a setpoint carefully and ensure complete conversion at that temperature. However, this interference would only be significant during nighttime or during very cold weather sampling. N_2O_5 is not typically considered in the TD NO_2 instrument literature because the existing instruments have largely operated in the daytime, when concentrations of N_2O_5 are not a significant fraction of NO_x . The first dissociation is approximately quantitative at the oven set temperatures used to quantify PN, with the second dissociation occurring at temperatures used for HNO_3 detection. However, this interference would only be significant during nighttime or during very cold weather sampling and is already accounted for in the analysis of these instruments. (Slusher et al., 2004; Thieser et al., 2016)~~

The thermogram of particulate ammonium nitrate matches the thermogram of HNO_3 , within the margin of error of the UHSAS measurement. TD ovens have not typically been used explicitly for particle detection, with a few exceptions (Voisin et al., 2003; Smith et al., 2004; Rollins et al., 2010). ~~though F very fine particles likely will may be sampled by the inlet, unless they are excluded aerodynamically or physically. These results demonstrate that the volatile portion of the particulate ammonium nitrates will be driven into the gas phase at low oven temperatures, consistent with Rollins et al. (2010), who used a denuder to remove gas phase nitrates and to detect aerosol organic nitrates in a 325 °C oven. Their results indicate it is likely that particulate organic nitrates would be converted to NO_2 with 100% efficiency in the NOAA TD-CRDS, but this result has not been explicitly tested here.~~ Other NO_3 salts might also be detected via thermal dissociation, although it is expected that they would be non-volatile at the temperatures of these TD-inlets. Bertram and Cohen (2003) examined NaNO_3 and determined that those particles would not be detected in TD inlets. However, these studies measured pure aerosols, and results may vary with heterogeneously mixed particles with multiple components. The initial dissociation of NH_4NO_3 will produce an NH_3 molecule in addition to an HNO_3 molecule, which means that particles may be subject to the same NH_3/O_3 interference when sampling in ambient air, which was not considered in this study. Additionally, the particles sampled in this paper were generated and injected directly into the inlet. The efficiency of particle sampling in ambient air will depend on particle size and inlet design,

Formatted: Subscript
Formatted: Subscript

Formatted: Subscript

particularly during aircraft measurements. In future studies, a TD inlet that either effectively samples aerosol, or effectively excludes aerosol (such as a cyclone), or a combination of the two could be used to specifically measure aerosol nitrates, which may make up a substantial fraction of NO_y, particularly in polluted wintertime urban atmospheres.

Formatted: Subscript

5 Based on the results of this paper, we make the following three recommendations: (1) TD ovens should be calibrated characterized with the appropriate reactive nitrogen compounds regularly at the oven set points using the oven residence time and gas pressure that will be used in ambient sampling. This is especially important given the findings of the Berkeley group regarding impurities found in otherwise identical ovens, as discussed in Sect. 3.1. (2) In addition to the AN and PN calibrations recommended by
10 (Day et al., 2002; Thieser et al., 2016) and others, these calibrations should include HNO₃. HNO₃ calibration will be especially important if sampling in regions where HNO₃ is in large excess over other NO_y species. (3) Potential non-NO_y species such as NH₃ should also be regularly introduced into the inlet under conditions where O₃ is present in ambient air to check for potential conversion. These recommendations are similar to those detailed in Bradshaw et al. (1998). The results of Fig. 9 indicate that
15 calibration results may also vary significantly when sampling in ambient air, due to the large number of possible gas-phase reactions available to the wide variety of trace atmospheric species. The last step is particularly important in instruments that detect NO as well as NO₂. Comprehensive calibration of these instruments NO_y measurement accuracy, which in turn will provide valuable information about tropospheric NO_x chemistry.

20 Acknowledgements

We would like to thank Douglas Day for his advice on the construction and deployment of TD inlets, and Jim Roberts, Tom Ryerson, Dave Parrish, and Joel Thornton for other helpful discussions. We also wish to thank Jessica Gilman for providing the GC/MS VOC mixture, Sascha Albrecht for measuring the NO₂ baseline in the HNO₃ permeation tube, and Jim Burkholder for the loan of a propane tank. CCW
25 acknowledges support from the National Research Council Research Associateship Program. The authors acknowledge support from the Atmospheric Chemistry, Carbon Cycle and Climate Program (AC4).

References

30 Beaver, M. R., Clair, J. M. S., Paulot, F., Spencer, K. M., Crounse, J. D., LaFranchi, B. W., Min, K. E., Pusede, S. E., Wooldridge, P. J., Schade, G. W., Park, C., Cohen, R. C., and Wennberg, P. O.: Importance of biogenic precursors to the budget of organic nitrates: observations of multifunctional organic nitrates by CIMS and TD-LIF during BEARPEX 2009, *Atmos. Chem. Phys.*, 12, 5773-5785, 10.5194/acp-12-5773-2012, 2012.

Bertram, T. H., and Cohen, R. C.: A prototype instrument for the real time detection of semi-volatile organic and inorganic nitrate aerosol, *Eos Trans. AGU*, 84(46), Fall Meet. Suppl., Abstract A51F-0740, 2003,

Bertram, T. H., Thornton, J. A., and Riedel, T. P.: An experimental technique for the direct measurement of N_2O_5 reactivity on ambient particles, *Atmos. Meas. Tech.*, 2, 231-242, 10.5194/amt-2-231-2009, 2009.

5 Bradshaw, J., Sandholm, S., and Talbot, R.: An update on reactive odd-nitrogen measurements made during recent NASA Global Tropospheric Experiment programs, *J. Geophys. Res. - Atmos.*, 103, 19129-19148, 10.1029/98JD00621, 1998.

10 Cai, Y., Montague, D. C., Mooiweer-Bryan, W., and Deshler, T.: Performance characteristics of the ultra high sensitivity aerosol spectrometer for particles between 55 and 800 nm: Laboratory and field studies, *J. Aerosol Sci.*, 39, 759-769, 10.1016/j.jaerosci.2008.04.007, 2008.

Cohen, R. C.: Private communication, WINTER data workshop, 2016.

15 Crosley, D. R.: NO_y Blue Ribbon panel, *J. Geophys. Res. - Atmos.*, 101, 2049-2052, 10.1029/95JD02276, 1996.

Darley, E. F., Kettner, K. A., and Stephens, E. R.: Analysis of peroxyacetyl nitrates by gas chromatography with electron capture detection, *Anal. Chem.*, 35, 589-591, 10.1021/ac60197a028, 1963.

20 Davidson, J. A., Viggiano, A. A., Howard, C. J., Dotan, I., Fehsenfeld, F. C., Albritton, D. L., and Ferguson, E. E.: Rate constants for the reactions of O_2^+ , NO_2^+ , NO^+ , H_3O^+ , CO_3^- , NO_2^- , and halide ions with N_2O_5 at 300 K, *J. Chem. Phys.*, 68, 2085-2087, 10.1063/1.436032, 1978.

25 Day, D. A., Wooldridge, P. J., Dillon, M. B., Thornton, J. A., and Cohen, R. C.: A thermal dissociation laser-induced fluorescence instrument for in situ detection of NO_2 , peroxy nitrates, alkyl nitrates, and HNO_3 , *J. Geophys. Res.*, 107, 10.1029/2001jd000779, 2002.

30 Day, D. A., Dillon, M. B., Wooldridge, P. J., Thornton, J. A., Rosen, R. S., Wood, E. C., and Cohen, R. C.: On alkyl nitrates, O_3 , and the “missing NO_y ”, *J. Geophys. Res.*, 108, 10.1029/2003jd003685, 2003.

DeCarlo, P. F., Slowik, J. G., Worsnop, D. R., Davidovits, P., and Jimenez, J. L.: Particle morphology and density characterization by combined mobility and aerodynamic diameter measurements. Part 1: Theory, *Aerosol Sci. Tech.*, 38, 1185-1205, 10.1080/027868290903907, 2004.

35 Di Carlo, P., Aruffo, E., Busilacchio, M., Giammaria, F., Dari-Salisburgo, C., Biancofiore, F., Visconti, G., Lee, J., Moller, S., Reeves, C. E., Bauguitte, S., Forster, G., Jones, R. L., and Ouyang, B.: Aircraft based four-channel thermal dissociation laser induced fluorescence instrument for simultaneous measurements of $\text{NO}_{<2>}$, total peroxy nitrate, total alkyl nitrate, and $\text{HNO}_{<3>}$, *Atmos. Meas. Tech.*, 6, 971-980, 10.5194/amt-6-971-2013, 2013.

Dillon, M. B., Lamanna, M. S., Schade, G. W., Goldstein, A. H., and Cohen, R. C.: Chemical evolution of the Sacramento urban plume: Transport and oxidation, *J. Geophys. Res. - Atmos.*, 107, ACH 3-1-ACH 3-15, 10.1029/2001JD000969, 2002.

Dubé, W. P., Brown, S. S., Osthoff, H. D., Nunley, M. R., Ciciora, S. J., Paris, M. W., McLaughlin, R. J., and Ravishankara, A. R.: Aircraft instrument for simultaneous, in situ measurement of NO_3 and N_2O_5 via pulsed cavity ring-down spectroscopy, *Rev. Sci. Instrum.*, 77, 034101, 10.1063/1.2176058, 2006.

EPA: 8-Hour ozone nonattainment areas (2008 standard) in EPA Green Book, available at: http://www.epa.gov/airquality/greenbook/map8hr_2008.html, 2016.

40 Fahey, D. W., Eubank, C. S., Hübler, G., and Fehsenfeld, F. C.: Evaluation of a catalytic reduction technique for the measurement of total reactive odd-nitrogen NO_y in the atmosphere, *J. Atmos. Chem.*, 3, 435-468, 10.1007/bf00053871, 1985.

Fahey, D. W., Hübler, G., Parrish, D. D., Williams, E. J., Norton, R. B., Ridley, B. A., Singh, H. B., Liu, S. C., and Fehsenfeld, F. C.: Reactive nitrogen species in the troposphere: Measurements of NO , NO_2HNO_3 , particulate nitrate, peroxyacetyl nitrate (PAN), O_3 , and total reactive odd nitrogen (NO_y) at Niwot Ridge, Colorado, *J. Geophys. Res.*, 91, 9781-9793, 1986.

45 Fehsenfeld, F. C., Huey, L. G., Sueper, D. T., Norton, R. B., Williams, E. J., Eisele, F. L., Mauldin, R. L., and Tanner, D. J.: Ground-based intercomparison of nitric acid measurement techniques, *J. Geophys. Res. - Atmos.*, 103, 3343-3353, 10.1029/97JD02213, 1998.

Flocke, F. M., Weinheimer, A. J., Swanson, A. L., Roberts, J. M., Schmitt, R., and Shertz, S.: On the measurement of PANs by gas chromatography and electron capture detection, *J. Atmos. Chem.*, 52, 19-43, 10.1007/s10874-005-6772-0, 2005.

Fuchs, H., Dubé, W. P., Lerner, B. M., Wagner, N. L., Williams, E. J., and Brown, S. S.: A sensitive and 5 versatile detector for atmospheric NO₂ and NO_x based on blue diode laser cavity ring-down spectroscopy, *Environ. Sci. Technol.*, 43, 7831-7836, 10.1021/es902067h, 2009.

Glänzer, K., and Troe, J.: Thermal decomposition of nitrocompounds in shock waves. IV: Decomposition of nitric acid, *Berich. Bunsen. Gesell.*, 78, 71-76, 10.1002/bbpc.19740780112, 1974.

Huey, L. G., Dunlea, E. J., Lovejoy, E. R., Hanson, D. R., Norton, R. B., Fehsenfeld, F. C., and Howard, C. J.: Fast time response measurements of HNO₃ in air with a chemical ionization mass spectrometer, *J. Geophys. Res - Atmos.*, 103, 3355-3360, 10.1029/97JD02214, 1998.

Huey, L. G.: Measurement of trace atmospheric species by chemical ionization mass spectrometry: Speciation of reactive nitrogen and future directions, *Mass Spectrom. Rev.*, 26, 166-184, 10.1002/mas.20118, 2007.

Johnston, H. S., Cantrell, C. A., and Calvert, J. G.: Unimolecular decomposition of NO₃ to form NO and O₂ and a review of N₂O₅/NO₃ kinetics, *J. Geophys. Res - Atmos.*, 91, 5159-5172, 10.1029/JD091iD04p05159, 1986.

Kercher, J. P., Riedel, T. P., and Thornton, J. A.: Chlorine activation by N₂O₅: simultaneous, in situ detection of ClNO₂ and N₂O₅ by chemical ionization mass spectrometry, *Atmos. Meas. Tech.*, 2, 193-204, 10.5194/amt-2-193-2009, 2009.

King, M. D., Dick, E. M., and Simpson, W. R.: A new method for the atmospheric detection of the nitrate radical (NO₃), *Atmos. Environ.*, 34, 685-688, [http://dx.doi.org/10.1016/S1352-2310\(99\)00418-5](http://dx.doi.org/10.1016/S1352-2310(99)00418-5), 2000.

Kley, D., and McFarland, M.: Chemiluminescence detector for NO and NO₂, *Atmospheric Technology*, 12, 63-69, 1980.

Kliner, D. A. V., Daube, B. C., Burley, J. D., and Wofsy, S. C.: Laboratory investigation of the catalytic reduction technique for measurement of atmospheric NO_y, *J. Geophys. Res - Atmos.*, 102, 10759-10776, 10.1029/96JD03816, 1997.

Lee, B. H., Lopez-Hilfiker, F. D., Mohr, C., Kurtén, T., Worsnop, D. R., and Thornton, J. A.: An iodide-adduct high-resolution time-of-flight chemical-ionization mass spectrometer: Application to atmospheric 30 inorganic and organic compounds, *Environ. Sci. Technol.*, 48, 6309-6317, 10.1021/es500362a, 2014.

Lee, B. H., Mohr, C., Lopez-Hilfiker, F. D., Lutz, A., Hallquist, M., Lee, L., Romer, P., Cohen, R. C., Iyer, S., Kurtén, T., Hu, W., Day, D. A., Campuzano-Jost, P., Jimenez, J. L., Xu, L., Ng, N. L., Guo, H., Weber, R. J., Wild, R. J., Brown, S. S., Koss, A., de Gouw, J., Olson, K., Goldstein, A. H., Seco, R., Kim, S., McAvey, K., Shepson, P. B., Starn, T., Baumann, K., Edgerton, E. S., Liu, J., Shilling, J. E., Miller, D. O., Brune, W., Schobesberger, S., D'Ambro, E. L., and Thornton, J. A.: Highly functionalized organic nitrates in the southeast United States: Contribution to secondary organic aerosol and reactive nitrogen 35 budgets, *Proc. Natl. Acad. Sci. USA*, 113, 1516-1521, 10.1073/pnas.1508108113, 2016.

Manion, J. A., Huie, R. E., Levin, R. D., Jr., D. R. B., Orkin, V. L., Tsang, W., McGivern, W. S., Hudgens, J. W., Knyazev, V. D., Atkinson, D. B., Chai, E., Tereza, A. M., Lin, C.-Y., Allison, T. C., Mallard, W. G., Westley, F., Herron, J. T., Hampson, R. F., and Frizzell, D. H.: NIST Chemical Kinetics Database, NIST Standard Reference Database 17, Version 7.0 (Web Version), Release 1.6.8, Data version 2015.12, 2015.

Neuman, J. A., Huey, L. G., Ryerson, T. B., and Fahey, D. W.: Study of inlet materials for sampling 40 atmospheric nitric acid, *Environ. Sci. Technol.*, 33, 1133-1136, 10.1021/es980767f, 1999.

Neuman, J. A., Huey, L. G., Dissly, R. W., Fehsenfeld, F. C., Flocke, F., Holecek, J. C., Holloway, J. S., Hübner, G., Jakoubek, R., Nicks, D. K., Parrish, D. D., Ryerson, T. B., Sueper, D. T., and Weinheimer, A. J.: Fast-response airborne in situ measurements of HNO₃ during the Texas 2000 Air Quality Study, *J. Geophys. Res - Atmos.*, 107, 4436, 10.1029/2001JD001437, 2002.

Neuman, J. A., Ryerson, T. B., Huey, L. G., Jakoubek, R., Nowak, J. B., Simons, C., and Fehsenfeld, F. C.: Calibration and evaluation of nitric acid and ammonia permeation tubes by UV optical absorption, *Environ. Sci. Technol.*, 37, 2975, 10.1021/es026422l, 2003.

5 Neuman, J. A., Aikin, K. C., Atlas, E. L., Blake, D. R., Holloway, J. S., Meinardi, S., Nowak, J. B., Parrish, D. D., Peischl, J., Perring, A. E., Pollack, I. B., Roberts, J. M., Ryerson, T. B., and Trainer, M.: Ozone and alkyl nitrate formation from the Deepwater Horizon oil spill atmospheric emissions, *J. Geophys. Res. - Atmos.*, 117, D09305, 10.1029/2011JD017150, 2012.

10 Nikitas, C., Clemithshaw, K. C., Oram, D. E., and Penkett, S. A.: Measurement of PAN in the polluted boundary layer and free troposphere using a luminol-NO₂ detector combined with a thermal converter, *J. Atmos. Chem.*, 28, 339-359, 10.1023/A:1005898017520, 1997.

15 O'Brien, J. M., Shepson, P. B., Muthuramu, K., Hao, C., Niki, H., Hastie, D. R., Taylor, R., and Roussel, P. B.: Measurements of alkyl and multifunctional organic nitrates at a rural site in Ontario, *J. Geophys. Res. - Atmos.*, 100, 22795-22804, 10.1029/94JD03247, 1995.

15 O'Keefe, A., and Deacon, D. A. G.: Cavity ring-down optical spectrometer for absorption measurements using pulsed laser sources, *Rev. Sci. Instrum.*, 59, 2544-2551, 10.1063/1.1139895, 1988.

20 Paul, D., Furgeson, A., and Osthoff, H. D.: Measurements of total peroxy and alkyl nitrate abundances in laboratory-generated gas samples by thermal dissociation cavity ring-down spectroscopy, *Rev. Sci. Instrum.*, 80, 114101, 10.1063/1.3258204, 2009.

25 Pérez, I. M., Wooldridge, P. J., and Cohen, R. C.: Laboratory evaluation of a novel thermal dissociation chemiluminescence method for in situ detection of nitrous acid, *Atmos. Environ.*, 41, 3993-4001, <http://dx.doi.org/10.1016/j.atmosenv.2007.01.060>, 2007.

Perner, D., and Platt, U.: Detection of nitrous acid in the atmosphere by differential optical absorption, *Geophysical Research Letters*, 6, 917-920, 10.1029/GL006i012p00917, 1979.

30 Phillips, G. J., Pouvesle, N., Thieser, J., Schuster, G., Axinte, R., Fischer, H., Williams, J., Lelieveld, J., and Crowley, J. N.: Peroxyacetyl nitrate (PAN) and peroxyacetic acid (PAA) measurements by iodide chemical ionisation mass spectrometry: first analysis of results in the boreal forest and implications for the measurement of PAN fluxes, *Atmos. Chem. Phys.*, 13, 1129-1139, 10.5194/acp-13-1129-2013, 2013.

35 Pusede, S. E., Duffey, K. C., Shusterman, A. A., Saleh, A., Laughner, J. L., Wooldridge, P. J., Zhang, Q., Parworth, C. L., Kim, H., Capps, S. L., Valin, L. C., Cappa, C. D., Fried, A., Walega, J., Nowak, J. B., Weinheimer, A. J., Hoff, R. M., Berkoff, T. A., Beyersdorf, A. J., Olson, J., Crawford, J. H., and Cohen, R. C.: On the effectiveness of nitrogen oxide reductions as a control over ammonium nitrate aerosol, *Atmos. Chem. Phys.*, 16, 2575-2596, 10.5194/acp-16-2575-2016, 2016.

40 Ridley, B. A., and Howlett, L. C.: An instrument for nitric oxide measurements in the stratosphere, *Rev. Sci. Instrum.*, 45, 742-746, doi:<http://dx.doi.org/10.1063/1.1686726>, 1974.

45 Rollins, A. W., Smith, J. D., Wilson, K. R., and Cohen, R. C.: Real time in situ detection of organic nitrates in atmospheric aerosols, *Environ. Sci. Technol.*, 44, 5540-5545, 10.1021/es100926x, 2010.

Sadanaga, Y., Takaji, R., Ishiyama, A., Nakajima, K., Matsuki, A., and Bandow, H.: Thermal dissociation cavity attenuated phase shift spectroscopy for continuous measurement of total peroxy and organic nitrates in the clean atmosphere, *Rev. Sci. Instrum.*, 87, 074102, doi:<http://dx.doi.org/10.1063/1.4958167>, 2016.

50 Sander, S. P., Abbatt, J., Barker, J. R., Burkholder, J. B., Friedl, R. R., Golden, D. M., Huie, R. E., Kolb, C. E., Kurylo, M. J., Moortgat, G. K., Orkin, V. L., and Wine, P. H.: Chemical kinetics and photochemical data for use in atmospheric studies. Evaluation No. 17 (<http://ipldataeval.jpl.nasa.gov/>), 2011.

Schott, G., and Davidson, N.: Shock waves in chemical kinetics: The decomposition of N₂O₅ at high temperatures, *J. Am. Chem. Soc.*, 80, 1841-1853, 10.1021/ja01541a019, 1958.

Slusher, D. L., Huey, L. G., Tanner, D. J., Flocke, F. M., and Roberts, J. M.: A thermal dissociation-chemical ionization mass spectrometry (TD-CIMS) technique for the simultaneous measurement of peroxyacetyl nitrates and dinitrogen pentoxide, *J. Geophys. Res. - Atmos.*, 109, D19315, 10.1029/2004JD004670, 2004.

Smith, J. N., Moore, K. F., McMurry, P. H., and Eisele, F. L.: Atmospheric measurements of sub-20 nm diameter particle chemical composition by thermal desorption chemical ionization mass spectrometry, *Aerosol Sci. Tech.*, 38, 100-110, 10.1080/02786820490249036, 2004.

5 Sobanski, N., Schuladen, J., Schuster, G., Lelieveld, J., and Crowley, J.: A 5-channel cavity ring-down spectrometer for the detection of NO_2 , NO_3 , N_2O_5 , total peroxy nitrates and total alkyl nitrates, *Atmos. Meas. Tech. Discuss.*, 2016, 1-32, 10.5194/amt-2016-191, 2016.

Talbot, R. W., Vijgen, A. S., and Harriss, R. C.: Measuring tropospheric HNO_3 : Problems and prospects for nylon filter and mist chamber techniques, *J. Geophys. Res. - Atmos.*, 95, 7553-7561, 10.1029/JD095iD06p07553, 1990.

10 Thaler, R. D., Mielke, L. H., and Osthoff, H. D.: Quantification of nitryl chloride at part per trillion mixing ratios by thermal dissociation cavity ring-down spectroscopy, *Anal. Chem.*, 83, 2761-2766, 10.1021/ac200055z, 2011.

Thieser, J., Schuster, G., Schuladen, J., Phillips, G. J., Reiffs, A., Parchatka, U., Pöhler, D., Lelieveld, J., and Crowley, J. N.: A two-channel thermal dissociation cavity ring-down spectrometer for the detection of ambient NO_2 , RO_2NO_2 and RONO_2 , *Atmos. Meas. Tech.*, 9, 553-576, 10.5194/amt-9-553-2016, 2016.

15 Thornton, J. A., Wooldridge, P. J., and Cohen, R. C.: Atmospheric NO_2 : In situ laser-induced fluorescence detection at parts per trillion mixing ratios, *Anal. Chem.*, 72, 528-539, 10.1021/ac9908905, 2000.

Veres, P. R., Roberts, J. M., Wild, R. J., Edwards, P. M., Brown, S. S., Bates, T. S., Quinn, P. K., 20 Johnson, J. E., Zamora, R. J., and de Gouw, J.: Peroxynitric acid (HO_2NO_2) measurements during the UBWOS 2013 and 2014 studies using iodide ion chemical ionization mass spectrometry, *Atmos. Chem. Phys.*, 15, 8101-8114, 10.5194/acp-15-8101-2015, 2015.

25 Voisin, D., Smith, J. N., Sakurai, H., McMurry, P. H., and Eisele, F. L.: Thermal desorption chemical ionization mass spectrometer for ultrafine particle chemical composition, *Aerosol Sci. Tech.*, 37, 471-475, 10.1080/02786820300959, 2003.

Wagner, N. L., Dubé, W. P., Washenfelder, R. A., Young, C. J., Pollack, I. B., Ryerson, T. B., and Brown, S. S.: Diode laser-based cavity ring-down instrument for NO_3 , N_2O_5 , NO , NO_2 and O_3 from aircraft, *Atmos. Meas. Tech.*, 4, 1227-1240, 10.5194/amt-4-1227-2011, 2011.

30 Washenfelder, R. A., Wagner, N. L., Dubé, W. P., and Brown, S. S.: Measurement of atmospheric ozone by cavity ring-down spectroscopy, *Environ. Sci. Technol.*, 45, 2938-2944, 10.1021/es103340u, 2011.

Wild, R. J., Edwards, P. M., Dubé, W. P., Baumann, K., Edgerton, E. S., Quinn, P. K., Roberts, J. M., Rollins, A. W., Veres, P. R., Warneke, C., Williams, E. J., Yuan, B., and Brown, S. S.: A measurement of total reactive nitrogen, NO_y , together with NO_2 , NO , and O_3 via cavity ring-down spectroscopy, *Environ. Sci. Technol.*, 48, 9609-9615, 10.1021/es501896w, 2014.

35 Wild, R. J., Edwards, P. M., Bates, T. S., Cohen, R. C., de Gouw, J. A., Dubé, W. P., Gilman, J. B., Holloway, J., Kercher, J., Koss, A. R., Lee, L., Lerner, B. M., McLaren, R., Quinn, P. K., Roberts, J. M., Stutz, J., Thornton, J. A., Veres, P. R., Warneke, C., Williams, E., Young, C. J., Yuan, B., Zarzana, K. J., and Brown, S. S.: Reactive nitrogen partitioning and its relationship to winter ozone events in Utah, *Atmos. Chem. Phys.*, 16, 573-583, 10.5194/acp-16-573-2016, 2016.

40 Williams, E. J., Baumann, K., Roberts, J. M., Bertman, S. B., Norton, R. B., Fehsenfeld, F. C., Springston, S. R., Nunnermacker, L. J., Newman, L., Olszyna, K., Meagher, J., Hartsell, B., Edgerton, E., Pearson, J. R., and Rodgers, M. O.: Intercomparison of ground-based NO_y measurement techniques, *J. Geophys. Res. - Atmos.*, 103, 22261-22280, 10.1029/98JD00074, 1998.

45 Winer, A. M., Peters, J. W., Smith, J. P., and Pitts, J. N.: Response of commercial chemiluminescent nitric oxide-nitrogen dioxide analyzers to other nitrogen-containing compounds, *Environ. Sci. Technol.*, 8, 1118-1121, 10.1021/es60098a004, 1974.

50 Wooldridge, P. J., Perring, A. E., Bertram, T. H., Flocke, F. M., Roberts, J. M., Singh, H. B., Huey, L. G., Thornton, J. A., Wolfe, G. M., Murphy, J. G., Fry, J. L., Rollins, A. W., LaFranchi, B. W., and Cohen, R. C.: Total peroxy nitrates (ΣPNs) in the atmosphere: the Thermal Dissociation-Laser Induced Fluorescence (TD-LIF) technique and comparisons to speciated PAN measurements, *Atmos. Meas. Tech.*, 3, 593-607, 10.5194/amt-3-593-2010, 2010.

Worton, D. R., Mills, G. P., Oram, D. E., and Sturges, W. T.: Gas chromatography negative ion chemical ionization mass spectrometry: Application to the detection of alkyl nitrates and halocarbons in the atmosphere, *J. Chromatogr. A*, 1201, 112-119, <http://dx.doi.org/10.1016/j.chroma.2008.06.019>, 2008.

5 Xiong, F., McAvey, K. M., Pratt, K. A., Groff, C. J., Hostetler, M. A., Lipton, M. A., Starn, T. K., Seeley, J. V., Bertman, S. B., Teng, A. P., Crouse, J. D., Nguyen, T. B., Wennberg, P. O., Misztal, P. K., Goldstein, A. H., Guenther, A. B., Koss, A. R., Olson, K. F., de Gouw, J. A., Baumann, K., Edgerton, E. S., Feiner, P. A., Zhang, L., Miller, D. O., Brune, W. H., and Shepson, P. B.: Observation of isoprene hydroxynitrates in the southeastern United States and implications for the fate of NO_x , *Atmos. Chem. Phys.*, 15, 11257-11272, 10.5194/acp-15-11257-2015, 2015.

10 Zheng, W., Flocke, F. M., Tyndall, G. S., Swanson, A., Orlando, J. J., Roberts, J. M., Huey, L. G., and Tanner, D. J.: Characterization of a thermal decomposition chemical ionization mass spectrometer for the measurement of peroxy acyl nitrates (PANs) in the atmosphere, *Atmos. Chem. Phys.*, 11, 6529-6547, 10.5194/acp-11-6529-2011, 2011.

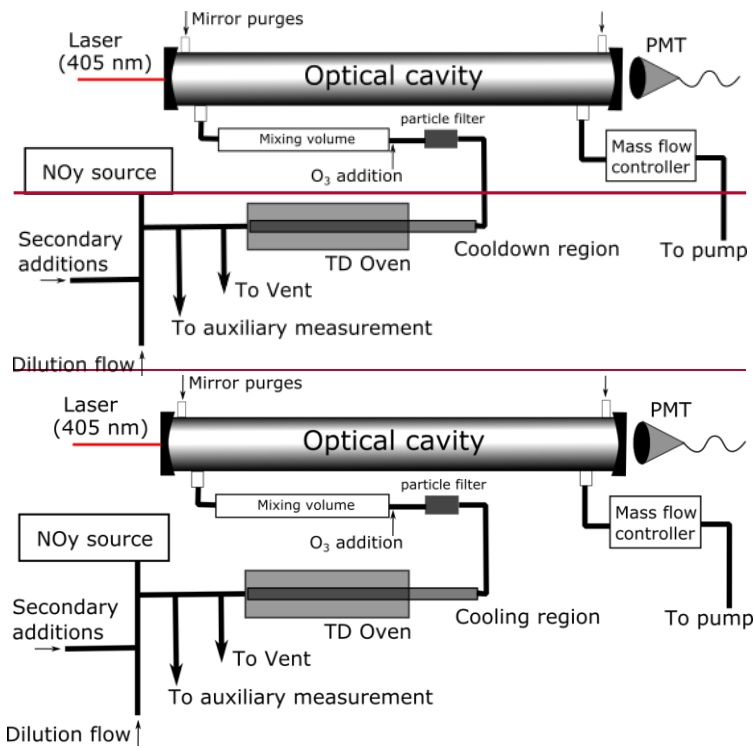
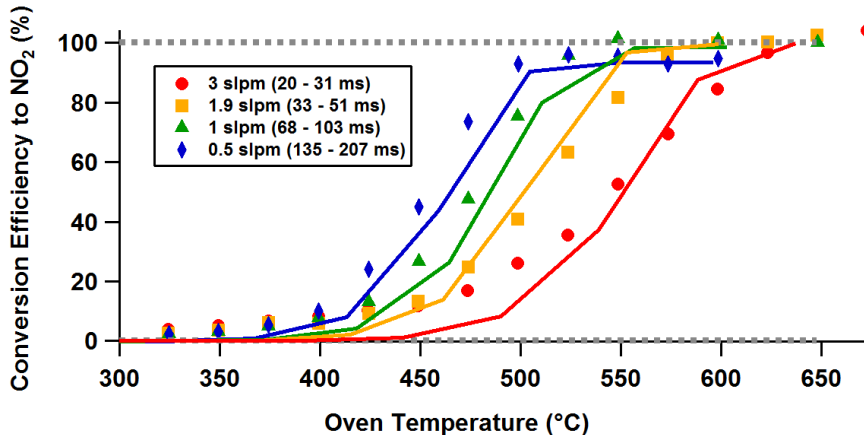
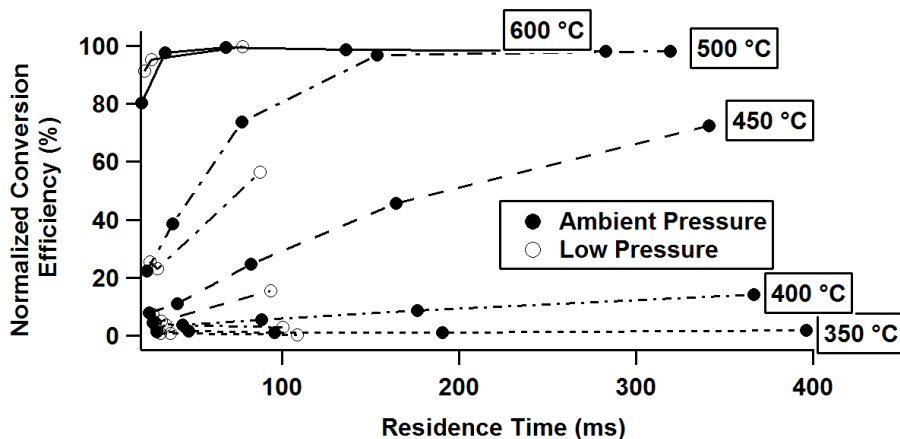


Figure 1: Instrument schematic of the TD-CRDS instrument used in this study. An NO_y source (HNO_3 permeation tube, N_2O_5 cold trap, NH_4NO_3 particle atomizer + DMA size-selector, or NH_3 permeation tube) is diluted by a zero air flow (with an option for adding O_3 , VOCs, RH, or CO through the secondary addition port), and passed through the TD oven. A portion of the flow is sampled prior to entering the oven with one of several type of auxiliary measurement (I- CIMS for N_2O_5 , UHSAS for NH_4NO_3 particles, or commercial CRDS for NH_3). After flowing through a cooling down-region, the

sample passes through a particle filter and then is mixed with a ~30 ppmv addition of O_3 in a mixing volume before entering through the optical cavity, where NO_2 is measured by CRDS.



| 5 Figure 2. HNO_3 thermograms measured at several flow rates in the NOAA TD-CRDS. Conversion efficiency is calculated as measured NO_2 signal relative to the expected concentration of HNO_3 . Parentheses in the legend indicate the range of residence times experienced by the sample in the heated inlet. The grey dashed lines indicate 0 and 100% conversion. Solid lines show simulations using a simple kinetic box model, as described in the text.



| 10 | 15 Figure 3. Conversion efficiencies of HNO_3 to NO_2 plotted as a function of plug flow residence times in the oven (see text) for 5 different temperatures. Values were obtained by scaling the measured conversion efficiency in Fig. 1 to the overall maximum and minimum of the thermogram, to account for slight differences between thermograms. Solid circles indicated measurements at ambient pressure, whereas open circles indicate measurements at low pressure. Different line traces indicated different temperatures. A temperature setpoint between 350 (small-short dashed line) and 450 degrees (long dashed line), and a residence time less than 200 ms are the conditions normally selected for selective detection of alkyl nitrates with no detection of HNO_3 . However, under these conditions HNO_3 conversion may be anywhere between 1 and 30%.

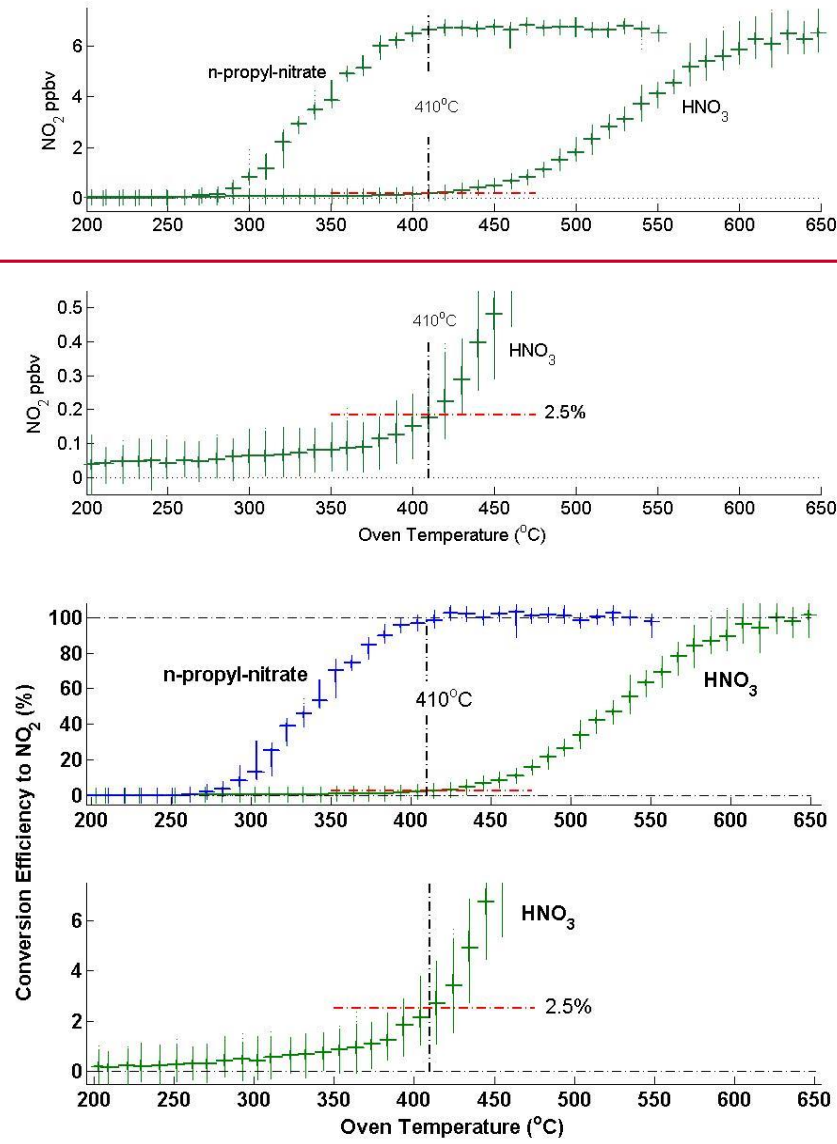


Figure 4. HNO_3 and *n*-propyl-nitrate thermograms taken with the Berkeley TD-LIF instrument used in the NASA DISCOVER-AQ California mission. The lower panel shows only HNO_3 with the y-axis expanded to illustrate the

dissociation onset. The oven is from the instrument's alkyl nitrates channel. The flow rate was approximately 2 slpm and the measurement setpoint was 410 °C. The dataset was corrected for the 2.5% dissociation of HNO₃ in the alkyl nitrates channel. A different **physical**-oven was used for HNO₃ at a setpoint of 620 °C.

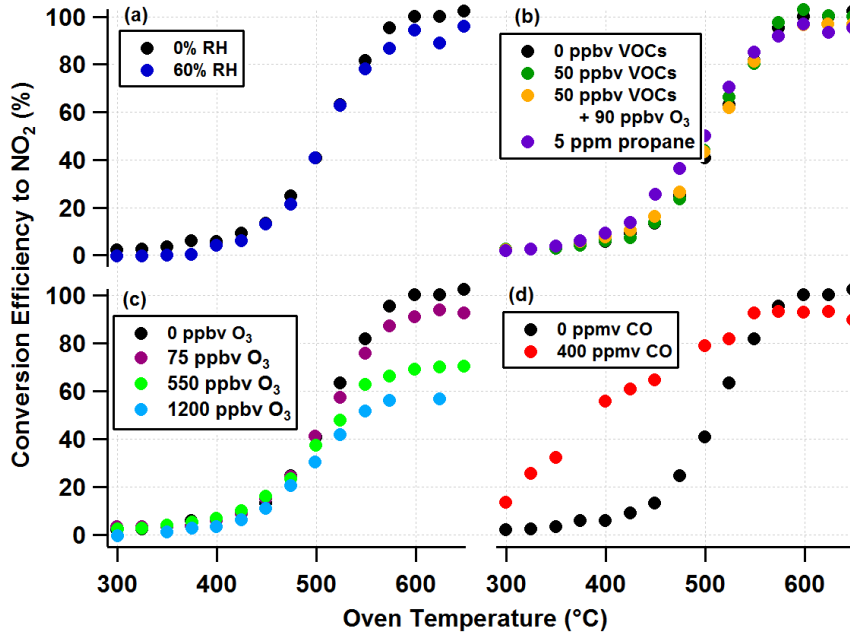


Figure 5. HNO₃ thermograms (1.9 slpm, ambient pressure) taken with the NOAA TD-CRDS, with various additions added prior to the TD oven. In each frame, the black solid circles indicate the no-addition case. In frames (a) and (b): No effect is observed when thermogram is taken at high relative humidity or when VOCs are added. In frame (c), varying amounts of O₃ were added, ranging from ambient levels (75 ppbv) to extremely polluted levels (1200 ppbv), which decreases the overall conversion at high temperatures. In frame (d), the addition of 400 ppmv CO alters the shape of the thermogram.

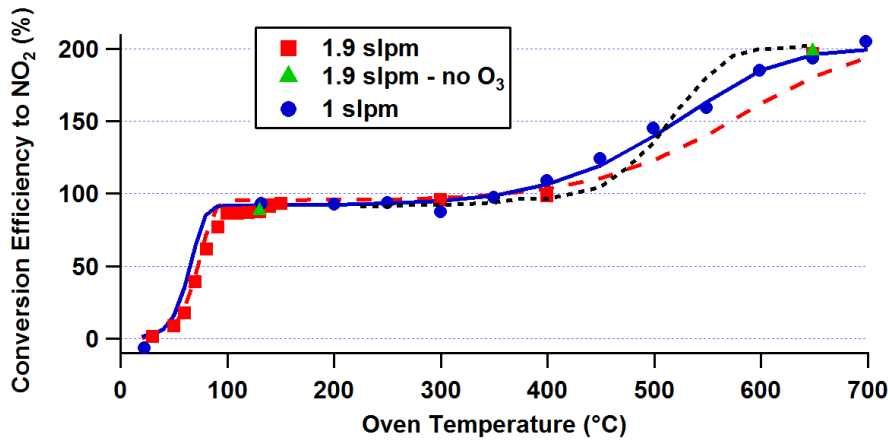


Figure 6. Thermogram of N_2O_5 measured in the NOAA TD-CRDS at two flow rates. The red squares and red dashed line show the 1.9 slpm thermogram and simulation, while the blue circles and blue solid line show the analogous result at 1.0 slpm. The first dissociation corresponds to $\text{N}_2\text{O}_5 \rightarrow \text{NO}_2 + \text{NO}_3$, and the second to $\text{NO}_3 \rightarrow \text{NO}_2 + \text{O}$. The second curve reaches a maximum of 200%, while the first reaches 90 – 95%, depending on the flow rate, due to recombination of NO_2 and NO_3 in the cooling region prior to the detector region. The black dashed line is the experimental HNO_3 thermogram from Fig. 2, offset by 100%. The green triangles indicate measurements of the conversion efficiency without the O_3 addition, confirming that the second dissociation must occur via $\text{NO}_3 \rightarrow \text{NO}_2 + \text{O}$ rather than $\text{NO}_3 \rightarrow \text{NO} + \text{O}_2$.

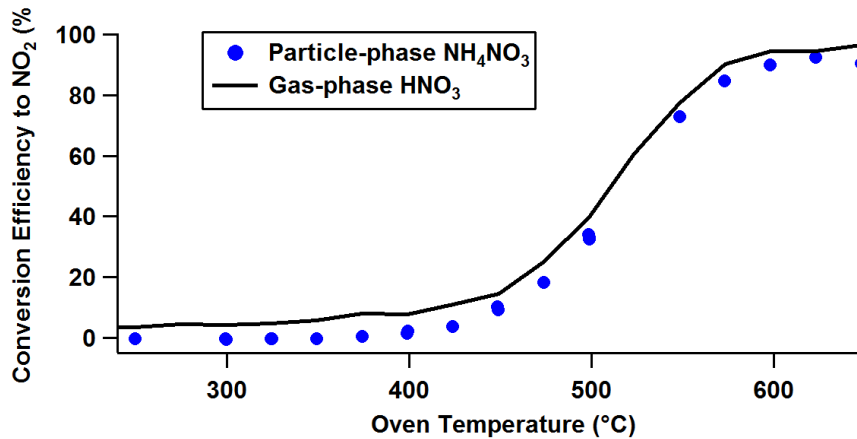


Figure 7. Measured thermogram of NH_4NO_3 particles as solid circles from the NOAA TD-CRDS. The black solid line indicates the measured thermogram of gas-phase HNO_3 at a 1.9 slpm flow rate (from the gold squares trace in Fig. 2). The close match of these two thermograms indicates that the NH_4NO_3 particles go through HNO_3 as an intermediate, and is a good indication that complete conversion is achieved.

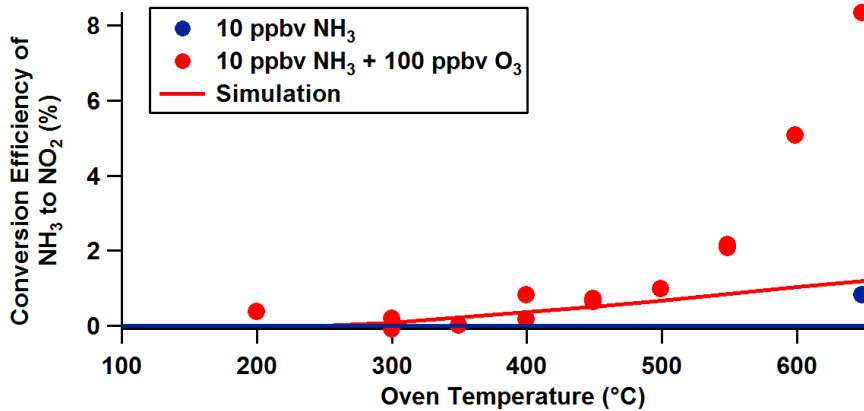


Figure 8. Thermogram of NH₃ taken with the NOAA TD-CRDS, with 100 ppbv of O₃ added before the oven shown in red circles. The blue circle represents an analogous measurement at 650 °C with no O₃ added. Kinetic box model simulations shown in solid lines of corresponding color.

5

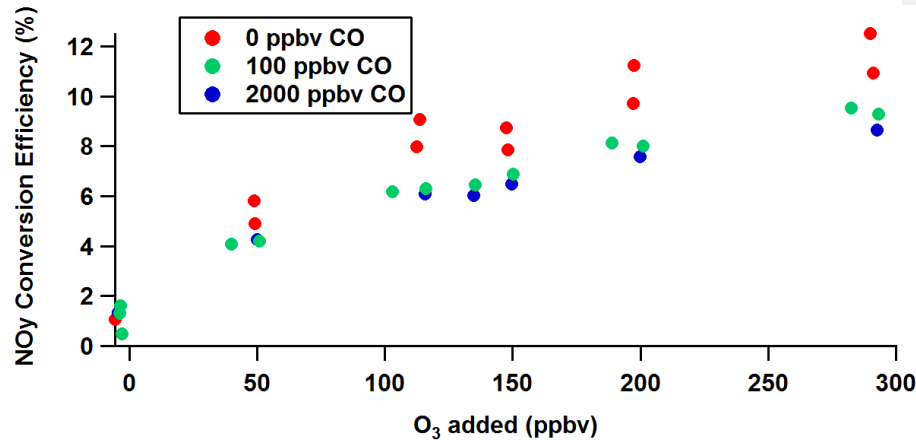


Figure 9. Conversion efficiency of NH₃ to NO_y as a function of O₃ added to the TD inlet. Red circles show 10 ppbv NH₃ with O₃ ranging from 0 – 300 ppbv, and the green and blue traces show similar data, but with 100 and 2000 ppbv CO added. The partial depletion of the signal (~25%) with the addition of CO indicates that the oxygen atoms formed from O₃ pyrolysis are preferentially reacting with CO instead of NH₃.

10

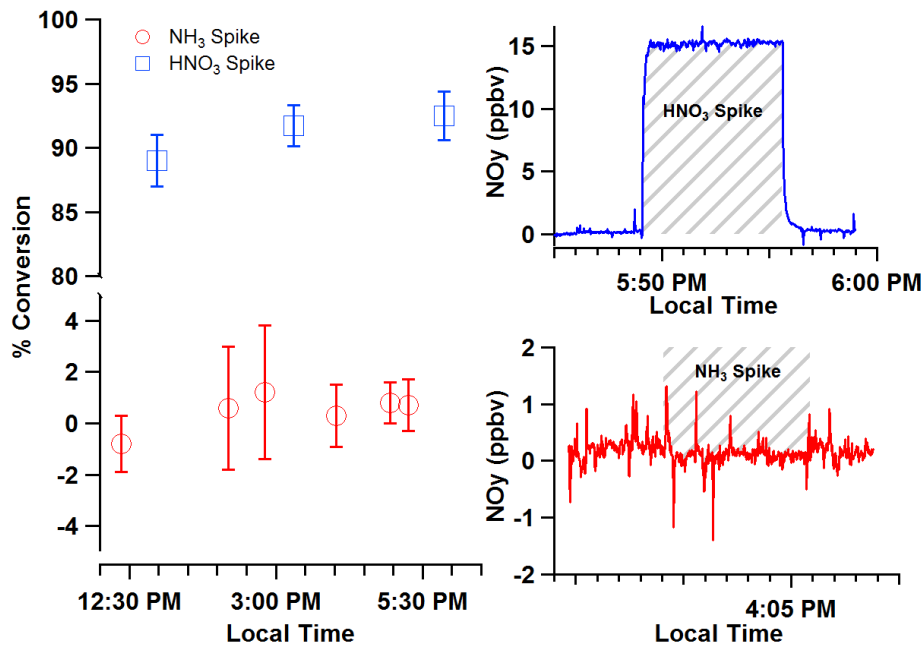


Figure 10. Measurement of HNO₃ and NH₃ conversion in ambient air at an inlet set temperature of 650 °C. The left panel shows measured conversion efficiencies for standard additions of HNO₃ and NH₃ to the NOAA TD-CRDS ~~an~~-inlet sampling ambient air in Boulder, CO on August 9, 2016. The right panels show time series of measured NO_y during standard additions. The data is the difference between two NO_y measurement channels, one with and one without the standard addition, to cancel the variation in ambient NO_y during the tests.